Developmental Biology 361 (2012) 12–26

Contents lists available at SciVerse ScienceDirect

Developmental Biology

journal homepage: www.elsevier.com/developmentalbiology

Multiple origins, migratory paths and molecular profiles of cells populating the avian interpeduncular nucleus

Beatriz Lorente-Cánovas [a,b], Faustino Marín [a], Rubén Corral-San-Miguel [a], Matías Hidalgo-Sánchez [c], José Luis Ferrán [a], Luis Puelles [a], Pilar Aroca [a,*]

[a] Department of Human Anatomy and Psychobiology; School of Medicine, University of Murcia, 30100 Murcia, Spain
[b] Wellcome Trust Sanger Institute, Wellcome Trust Genome Campus, Cambridge CB10 1SA, UK
[c] Department of Cell Biology, University of Extremadura, 06071 Badajoz, Spain

ARTICLE INFO

Article history:
Received for publication 17 May 2011
Revised 26 September 2011
Accepted 27 September 2011
Available online 12 October 2011

Keywords:
Interpeduncular nucleus
PAX7
Nkx6.1
Otp
Otx2
Cell migration
Isthmus
Rhombomere 1

ABSTRACT

The interpeduncular nucleus (IP) is a key limbic structure, highly conserved evolutionarily among vertebrates. The IP receives indirect input from limbic areas of the telencephalon, relayed by the habenula via the fasciculus retroflexus. The function of the habenulo-IP complex is poorly understood, although there is evidence that in rodents it modulates behaviors such as learning and memory, avoidance, reward and affective states. The IP has been an important subject of interest for neuroscientists, and there are multiple studies about the adult structure, chemoarchitecture and its connectivity, with complex results, due to the presence of multiple cell types across a variety of subnuclei. However, the ontogenetic origins of these populations have not been examined, and there is some controversy about its location in the midbrain-anterior hindbrain area. To address these issues, we first investigated the anteroposterior (AP) origin of the IP complex by fate-mapping its neuromeric origin in the chick, discovering that the IP develops strictly within isthmus and rhombomere 1. Next, we studied the dorsoventral (DV) positional identity of subpopulations of the IP complex. Our results indicate that there are at least four IP progenitor domains along the DV axis. These specific domains give rise to distinct subtypes of cell populations that target the IP with variable subnuclear specificity. Interestingly, these populations can be characterized by differential expression of the transcription factors Pax7, Nkx6.1, Otp, and Otx2. Each of these subpopulations follows a specific route of migration from its source, and all reach the IP roughly at the same stage. Remarkably, IP progenitor domains were found both in the alar and basal plates. Some IP populations showed rostrocaudal restriction in their origins (isthmus versus anterior or posterior r1 regions). A tentative developmental model of the structure of the avian IP is proposed. The IP emerges as a plurisegmental and developmentally heterogeneous formation that forms ventromedially within the isthmus and r1. These findings are relevant since they help to understand the highly complex chemoarchitecture, hodology and functions of this important brainstem structure.

© 2011 Elsevier Inc. All rights reserved.

Introduction

The interpeduncular nucleus (IP) is a highly conserved structure in all vertebrates, found subpially across the median floor plate of the brainstem at the posterior end of the interpeduncular fossa. The IP receives its major input from the medial habenula (mHb) via the fasciculus retroflexus (Contestabile and Flumerfelt, 1981; Herkenham and Nauta, 1979) and shows widespread projections, both ascending (to limbic structures) and descending (mainly to the raphe nuclei; Groenewegen et al., 1986).

Functional studies on the mHb-IP axis suggest its implication in a variety of brain functions and behaviors such as learning and memory, motor activity, stress, affective states (anxiety, depression, reward phenomena), as reviewed by Klemm (2004) and Hikosaka (2010). The IP consists of several cyto- and chemoarchitectonically distinct cell groups organized in a complex tridimensional structure (Hamill and Lenn, 1984; Hamill et al., 1984; Hemmendinger and Moore, 1984; Ives, 1971). Studies in mammals have addressed the diverse adult neurotransmitter phenotypes of its neurons and its projections to multiple brain areas, largely of the limbic system (e.g., Ferraguti et al., 1990; Groenewegen et al., 1986; Klemm, 2004; Nieuwenhuys et al., 1998; Panigrahy et al., 1998; Shibata and Suzuki, 1984; Shinoda et al., 1988).

* Corresponding author. Fax: +34 868883955.
E-mail addresses: bl2@sanger.ac.uk (B. Lorente-Cánovas), marin@um.es (F. Marín), ruben.corral@um.es (R. Corral-San-Miguel), mhidalgo@unex.es (M. Hidalgo-Sánchez), jlferran@um.es (J.L. Ferrán), puelles@um.es (L. Puelles), pilaroca@um.es (P. Aroca).

0012-1606/$ – see front matter © 2011 Elsevier Inc. All rights reserved.
doi:10.1016/j.ydbio.2011.09.032

It would be expected that subpopulations of the IP nuclear complex, differentially characterized by their neurotransmitter or peptide typology, or producing distinct projections, should be generated in different progenitor domains during development. However, the literature has not addressed to date the possible correlation of these cytochemical and hodologic subdivisions with embryological heterogeneity.

Concerning its adult topography, the location of the IP is still controversial, and it has been contradictorily attributed either to the midbrain (Hanaway et al., 1971; Panigrahy et al., 1998; Quina et al., 2009), to the rostral hindbrain (Herrick, 1934; His, 1892, 1895; Nieuwenhuys et al., 2008; Puelles et al., 2007; Ziehen, 1906) or even to the diencephalic tegmentum (Bayer and Altman, 2006).

Contemporaneous studies on the origin of spinal cord cell types have shown that positional patterning differences at the level of neuroepithelial progenitors arranged along the dorsoventral dimension of the neural tube wall underlie important aspects of neuronal subtype diversity. This occurs in the context of ventralizing and dorsalizing developmental instructive mechanisms that control differential molecular specification of the neuroepithelium (Briscoe and Ericson, 2001; Dessaud et al., 2010; Jessell, 2000; Shirasaki and Pfaff, 2002).

We have applied the same logic to analyze the developmental construction of the IP. Previous studies had shown that some subpopulations of the adult interpeduncular nucleus express *Pax7* (Stoykova and Gruss, 1994) or *Nkx6.1* (E. Puelles et al., 2001), these being transcription factors known to characterize different DV progenitor domains in the developing hindbrain. On the basis of these studies, our working hypothesis was that this nuclear complex might have multiple dorsoventral origins of its subpopulations.

In this study we focused on the origin and development of diverse molecularly characterized subpopulations of the chicken IP complex. The position of the mature IP subpially across the midline raises the question whether these cells originate locally at the floor plate domain, or migrate in from other longitudinal zones (basal or alar plates). We first addressed the potential existence of distinct progenitor domains for subpopulations of the IP, examining various molecular profiles and locating precisely the respective positions along the dorsoventral (DV) and anteroposterior (AP) axes. To this end, we first analyzed the expression pattern of the previously identified IP marker genes PAX7 and *Nkx6.1*, later adding to the analysis two other IP markers identified by us, *Otx2* and *Otp*. The analysis was performed at several embryonic stages of development, to illuminate apparent migration paths, and comparisons with DV and AP reference marker genes established the relative topography of both the progenitor domains and the migrating cells.

Recognition of specific differential molecular markers for the IP nucleus helped us also to address its controversial topology, using specific transcription factors serving as AP reference markers and quail-chick experimental fate mapping. To date, no other studies have analyzed in detail the development of this complex nucleus in any species. The present data provide the first experimental examination of the anteroposterior (AP) and dorsoventral (DV) origin of IP subnuclear populations in any vertebrate.

We identified four separate progenitor domains whose derivatives variously contribute to the IP complex; these each express differentially one of the analyzed transcription factors. It turns out that the IP integrates neuronal cohorts with separate alar versus basal, or rostral versus caudal, origins. It was possible to trace the migratory route of the respective derivatives into specific parts of the IP complex. Our data provide further evidence corroborating that positional molecular identity of the neural progenitors is an organizing principle underlying phenotypic diversity among the different neuronal subpopulations of a nuclear complex such as the IP. It is expected that present highlighting of developmental molecular diversity at the IP may help understand the alternative chemoanatomic and hodologic properties coexisting within this nuclear complex.

Materials and methods

Animals

All animals were treated according to the regulations and laws of the European Union (86/609/EEC) and the Spanish Government (Royal Decree 223/1998; revised Royal Decree 1021/2005) for the care and handling of animal in research. Fertilized chick (*Gallus gallus domesticus*) and quail (*Coturnix coturnix japonica*) eggs were incubated in a forced draft incubator at 38 °C. The stage of the embryos was established according to the Hamburger and Hamilton (1951) tables (stages HH). The embryo heads were fixed overnight in cold PFA 4% in PBS, and the brains were dissected before further processing.

Embryos to be sectioned with vibratome were previously embedded in 4% agarose in phosphate-buffered saline solution (PBS) and sectioned 100 μm-thick using a vibratome (data in Figs. 1–4A–D and 5) or, alternatively, dehydrated for paraffin embedding (results in Fig. 4E–L) or cryoprotected for cryostat sectioning (data in Fig. 6). The selected sectioning planes (transverse, horizontal or sagittal) referred specifically to r1, considering the axial incurvation caused by the cephalic flexure (Puelles et al., 2007). The sections were then processed for *in situ* hybridization and/or immunohistochemistry.

Embryos selected to be cryostat-sectioned were cryoprotected in 10% sucrose solution in PBS and embedded in 10% gelatin/10% sucrose solution in the same buffer. The blocks were frozen for 1 minute in −70 °C isopentane cooled on dry ice, and then stored at −80 °C. Cryostat serial sections 20 μm-thick were cut sagittal or transverse to r1, mounted as parallel sets on SuperFrost slides, and stored at −80 °C until used.

Quail-chick chimeras

Homotopic and isochronic quail-chick grafts of r1, r2 or isthmus were performed, using quail embryos as donors. The embryos were operated at stage HH10, and the chimeras where fixed at stages HH36–38 (10–12 days in ovo). The grafts affected one-half of the neural tube, and included different DV extents of the neural tube wall as judged from the dorsal midline, with some attached mesoderm. Some chimeras (such as chimera 1) were fixed overnight in 4% paraformaldehyde in PBS, and the heads were embedded in 4% agarose to obtain three parallel series of 80 μm-thick transverse sections; these were used for different *in situ* probes in comparable adjacent sections. Other chimeras (such as chimeras 2 and 3) were immersed overnight in Clarke's fixative, ulteriorly washed, dehydrated and embedded in paraffin, sectioned 12 μm-thick and mounted in two parallel series. One series was stained with cresyl violet for cytoarchitectural analysis, and the other was immunoreacted with anti-quail antibody (QCPN) (monoclonal mouse anti-quail antibody from the Developmental Studies Hybridoma Bank, Iowa University, Iowa City, IA). The QCPN selectively labels the cell nuclei of quail cells and thereby identifies the grafted tissue (labeled ventricular zone) and its derivatives (labeled mantle zone populations).

RNA probes

Digoxigenin-labeled riboprobes were synthesized from cDNAs kindly provided by other laboratories, as follows: *Dbh* and *ChAT* from H. Rohrer (Developmental Neurobiology, Max-Planck-Institute for Brain Research, Frankfurt, Germany), *Fgf8* from GR. Martin (Dept. of Anatomy and Program in Developmental Biology, University of California, San Francisco, CA USA), *Hoxa2* from R.J. Wingate (MRC Centre for Developmental Neurobiology, King's College London, Guy's Campus, London UK), *Phox2a* from J.F. Brunet and C. Goridis (Ecole Normale Supérieure, Département de Biologie, Paris, France), *Otp* and *Otx2* from A. Simeone (CEINGE Biotecnologie Avanzate,

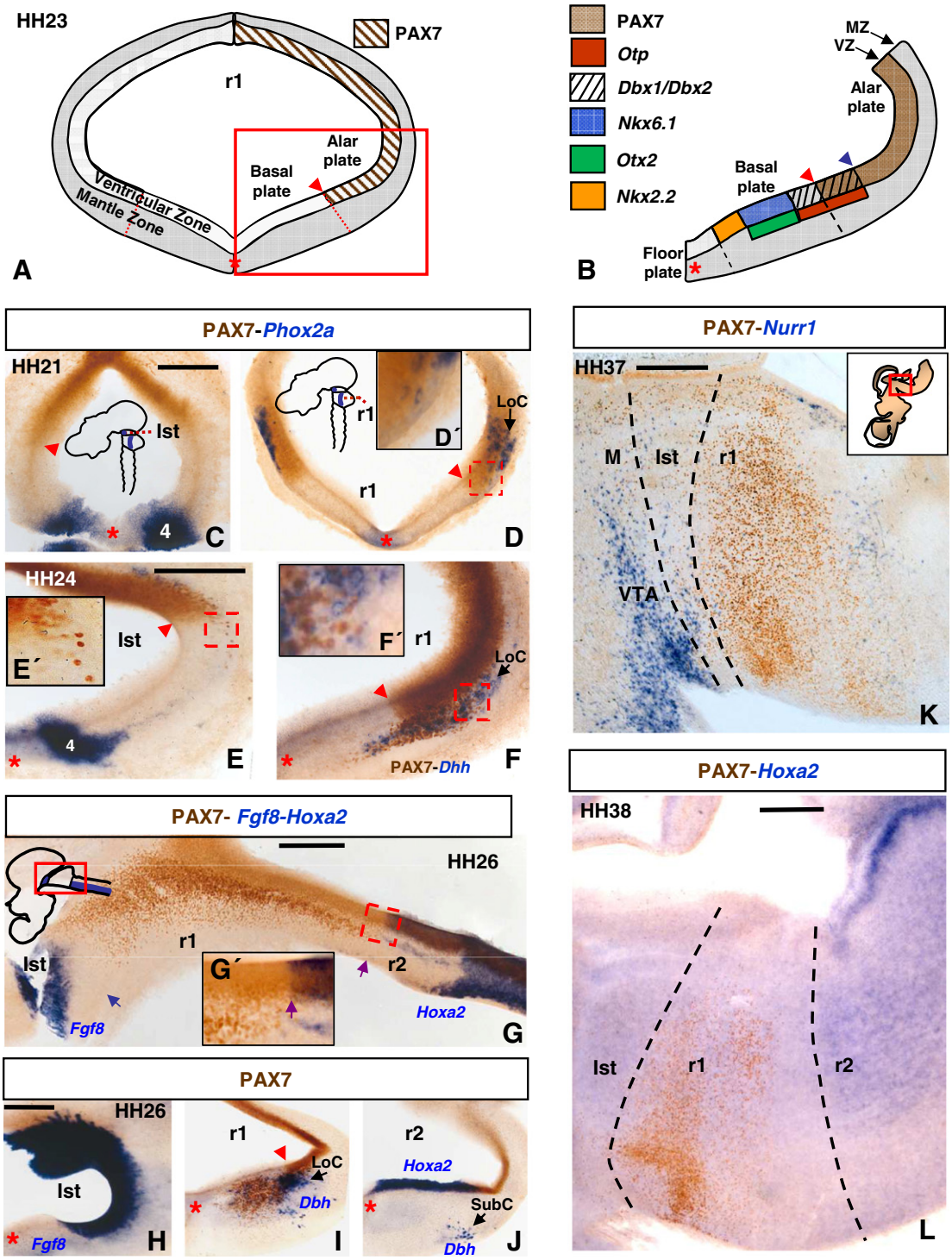

Fig. 1. Origin and localization of PAX7-positive migratory cells within r1. A, Schematic cross-section through r1 in a HH23 chick embryo showing PAX7 expression in the alar ventricular zone (VZ). The red box marks the area visualized in B and the transverse sections E, F, and H–J. B, Composite schema illustrating mutual relationships between the domains expressing the transcription factors selected in this work. PAX7-migratory cells are originated restrictedly in the VZ delimited between the red and blue arrowheads. C–F, Transverse sections at isthmus (C,E) and rhombomere 1 (D,F) levels, oriented as indicated in the diagrams in C and D, respectively, identify the earliest appearance of PAX7-positive cells in the mantle zone (MZ). *Phox2a* expression is used as a reference marker for isthmus and r1 (it labels trochlear motoneurons – 4 – at the isthmus and the locus coeruleus – LoC – at r1). Insets D′–F′ show enlarged views of the respective boxed areas. At HH24, the first PAX7-positive cells detach from the ventralmost part of the alar r1 VZ. G–J, Distribution of PAX7-positive cells in the r1 mantle zone at HH26. G, sagittal section showing PAX7-immunoreactive cells (brown) compared to *in situ* hybridization for *Fgf8* in the isthmus and for *Hoxa2* in r2 (both in blue). PAX7 cells are restricted to r1 and do not cross the boundaries with the isthmus or r2. G′ shows an enlarged view of the r1–r2 limit boxed in G (inset and arrow). H–J, Three transverse sections in rostrocaudal order, labeled with reference markers. PAX7-positive cells are restricted to the mantle of r1. H, The isthmus is strongly labeled with *Fgf8* and no PAX7 cells are present. I, PAX7-immunoreactive cells (brown) in r1 compared with *in situ* hybridization for dopamine-beta-hydroxylase (*Dbh*) (blue, expressed in LoC as a reference marker for r1). J, Expression of *Hoxa2* and *Dbh* (both in blue) are shown within r2 (*Dbh* in the subcoeruleus nucleus). *Hoxa2* is used as a reference marker for r2. Red arrowheads point to the alar–basal boundary at the VZ. Red asterisks indicate the floor plate. K–L, Parasagittal sections (from region boxed in the inset in K) showing double labeling with PAX7 antibody (brown) and *in situ* hybridization for either *Nurr1* or *Hoxa2* (both in blue). *Nurr1* (in K) and *Hoxa2* (in L) are used as reference markers for the rostral and caudal boundaries of r1, respectively. At HH37 and HH38, PAX7-positive cells are still restricted to r1. Scale bars = 200 μm.

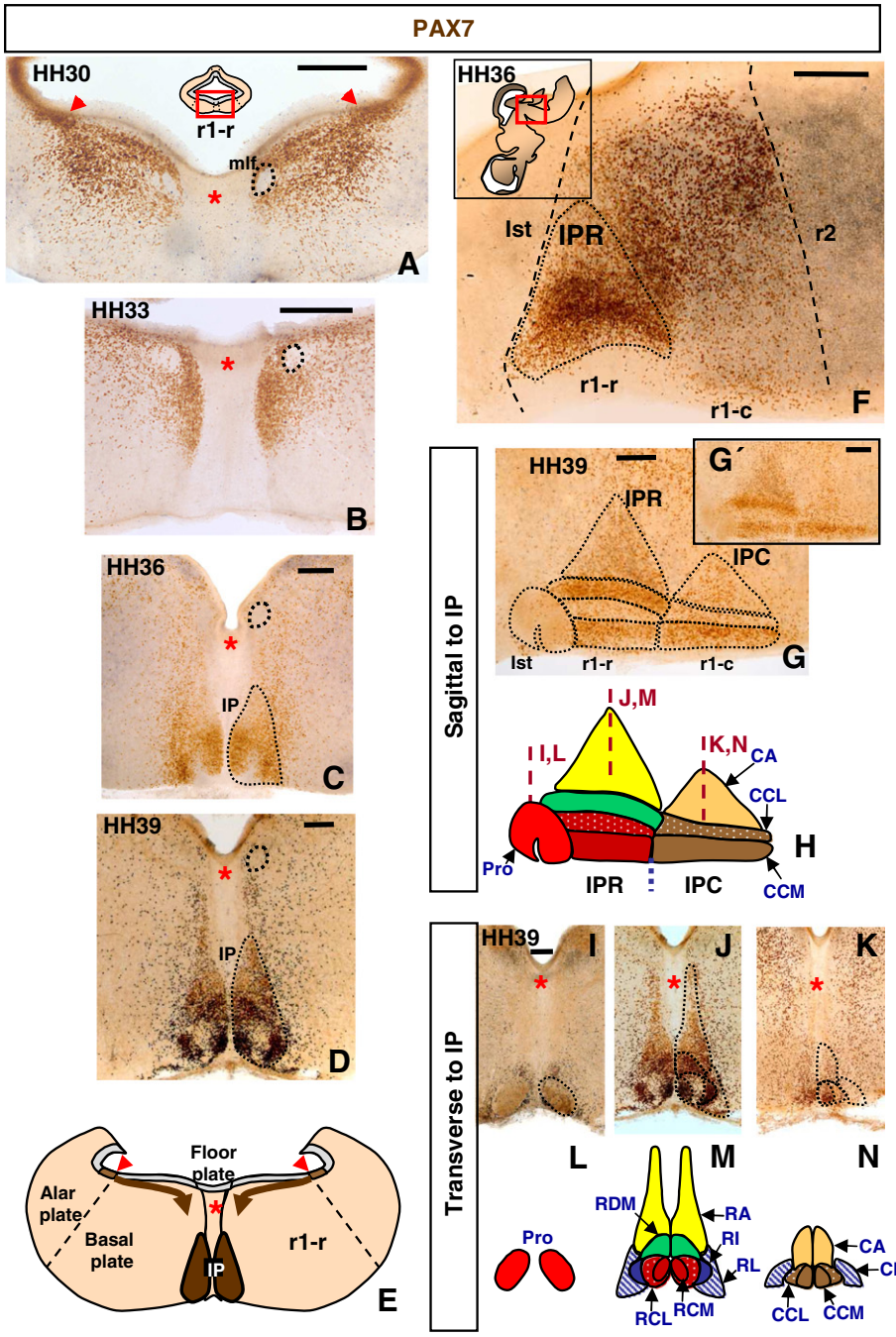

Fig. 2. Routes of migration and final fates of PAX7-positive cells in the IP. A–D, Distribution of PAX7-labeled cells (brown) at HH30, HH33, HH36 and HH39 in sections transverse to the rostral part of r1 (the diagram in A indicates the region shown in all transverse sections below). PAX7-positive cells enter a ventromedial subventricular migratory stream (A), continuing after a turn into a paramedian route (B) until they reach the subpial paramedian mantle (C), where they participate in forming the interpeduncular nucleus (D). E, Diagram depicting the origin, route and final destination of the PAX7-positive migratory population as inferred from our results. Red arrowheads indicate the alar-basal boundary at the VZ. F–G, PAX7 expression in paramedian sagittal sections at stages HH36 and HH39. There is a noticeable increase in the number of PAX7 cells traversing radially the mantle zone of the rostral part of r1 to reach the rostral part of IP (r1-r; IPR in F); similar cells reach later the caudal part of r1 to form part of the IP (r1-c; IPC in G). Note the lack of PAX7 expression in the Pro subdivision of the IP. The inset G' shows the same section without our interpretation. H, Schema of the inner structure of the three main rostrocaudal IP portions at HH39 (Pro, IPR and IPC), positioned at Ist, r1-r and r1-c levels, respectively (extrapolated from G). I–K, Selected transverse sections through Pro, IPR and IPC, respectively (section levels given in H) and labeled with PAX7 antibody to represent a map of IP subdivisions. L–N, Schematic cross-sections, illustrating the Pro, IPR and IPC (extrapolated from I–K). Note that IPR and IPC show a similar inner organization into core, dorsal and lateral shell-like portions (same color code is used for similar regions in H, L–N). See meaning of name tags for individual subnuclei in Abbreviations List. Red asterisks indicate the floor plate. Scale bars = 200 μm.

Naples, Italy), *Nkx6.1* and *Nkx2.2* were from J.L. Rubenstein (Department of Psychiatry and Nina Ireland Laboratory of Developmental Neurobiology, University of California, San Francisco, CA, USA). The cDNA of *Nurr1*, *Dbx1 and Dbx2* were obtained from the BBSRC Chick EST Database (Boardman et al., 2002).

In situ hybridization

Sagittal and transverse sections were processed for *in situ* hybridization using digoxigenin-labeled antisense RNA probes as described in Nieto et al.(1996). Alkaline phosphatase (AP)-conjugated anti-DIG

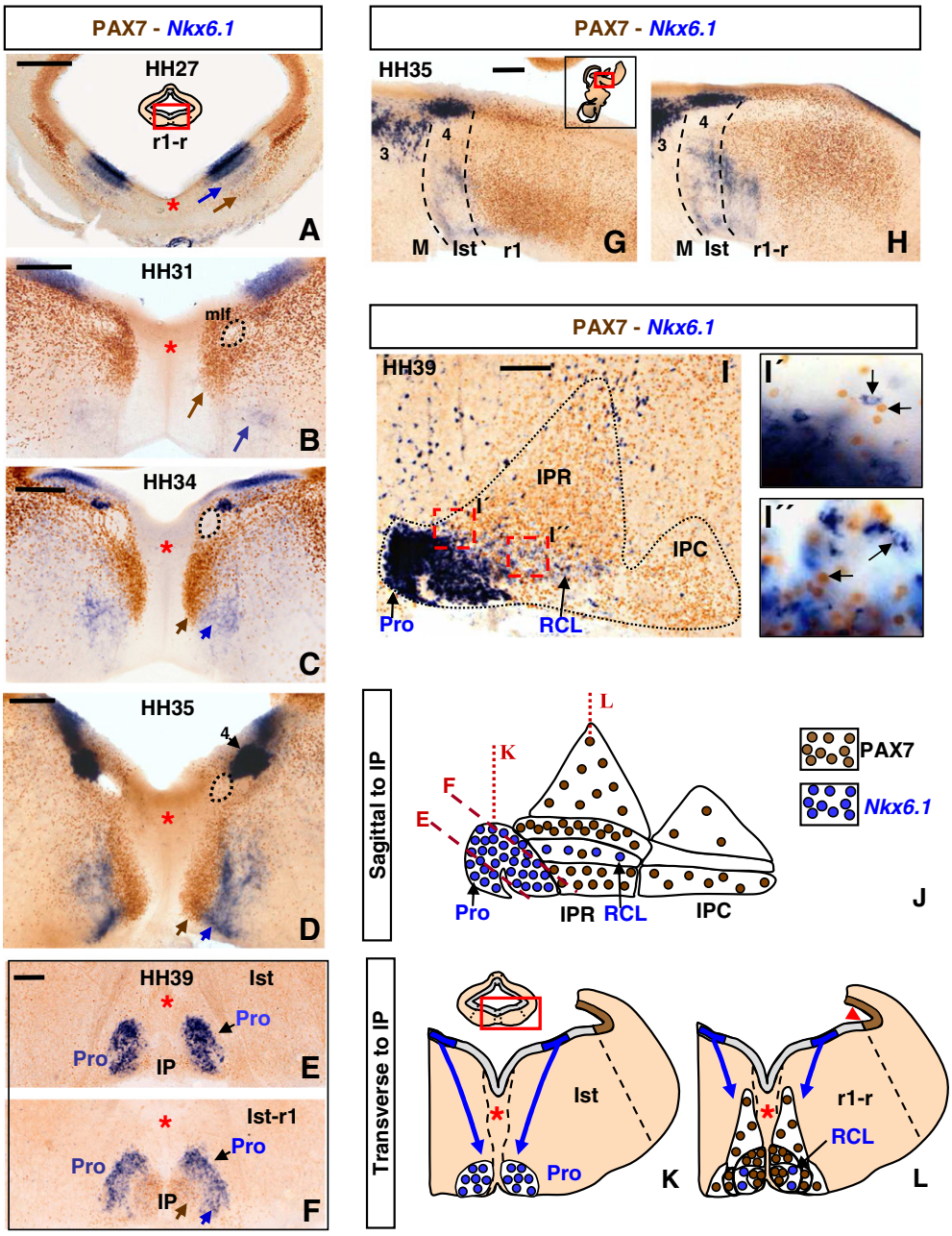

Fig. 3. Origin and final fate of *Nkx6.1*-positive cells in the IP. A–D, Transverse sections through rostral r1 (A-C) and Ist (D) (high-magnification of the area boxed in A), showing double staining with PAX7 antibody (brown) and *in situ* hybridization with *Nkx6.1* (blue) respectively at stages HH27, HH31, HH34 and HH35. Red asterisks indicate the floor plate. The brown and blue arrows point out the PAX7 and *Nkx6.1*-positive populations, respectively, which apparently follow parallel migratory routes. The two populations have different origins in the ventricular zone, but they converge upon the IP, roughly at the same time, at HH35 (D). E,F, Oblique coronal sections through IP at HH39 showing the population of *Nkx6.1* cells in the Pro subnucleus. The levels of these sections are indicated in J. G,H, Two adjacent paramedian sagittal sections of the rostral hindbrain (region boxed in G) at HH35, showing the AP extent of *Nkx6.1* signal at the isthmus and r1, compared to PAX7-labeled cells in r1. I, Distribution of *Nkx6.1*-positive and PAX7-positive cells in the IP at HH39. *Nkx6.1* is strongly expressed in the Pro subnucleus, though some scattered cells also appear in the RCL subnucleus of the IPR, as expected from earlier *Nkx6.1* expression in r1-r, shown in H. I′,I″ illustrate higher magnification of the areas boxed in I, highlighting the absence of cells coexpressing both markers (black arrows). J, Sagittal diagram of the IP nucleus indicating the distribution of *Nkx6.1*-cells (blue circles) with respect to PAX7-cells (brown circles). K,L, Schema showing the origin and final fate of *Nkx6.1*-positive cells (blue circles) at the isthmus and rostral-r1 levels, respectively (region boxed in K). The majority of migratory *Nkx6.1* cells form the Pro subdivision of the IP in the isthmus, while fewer cells enter the RCL in r1-r. Scale bars = 200 μm.

antibody was used thereafter (Roche Diagnostics, Mannheim, Germany; diluted 1:3500), and the NBT:BCIP substrates (Roche) were used to reveal the reaction in blue.

Immunocytochemistry

Floating vibratome sections were processed for immunohistochemistry either after ISH or independently. Antibodies used were monoclonal anti-PAX7 and anti-QCPN (Developmental Studies Hybridoma Bank; University of Iowa; dilutions 1:70 and 1:5, respectively). For ISH combined with immunocytochemistry, we first performed ISH without postfixing with paraformaldehyde, and then washed the sections with KTBT (50 mM Tris (pH 7.5), 150 mM NaCl, 10 mM KCl and 1% Triton X-100), before blocking in 20% sheep serum in KTBT. This was followed by incubation with primary antibody in KTBT. The sections were afterwards washed with KTBT and

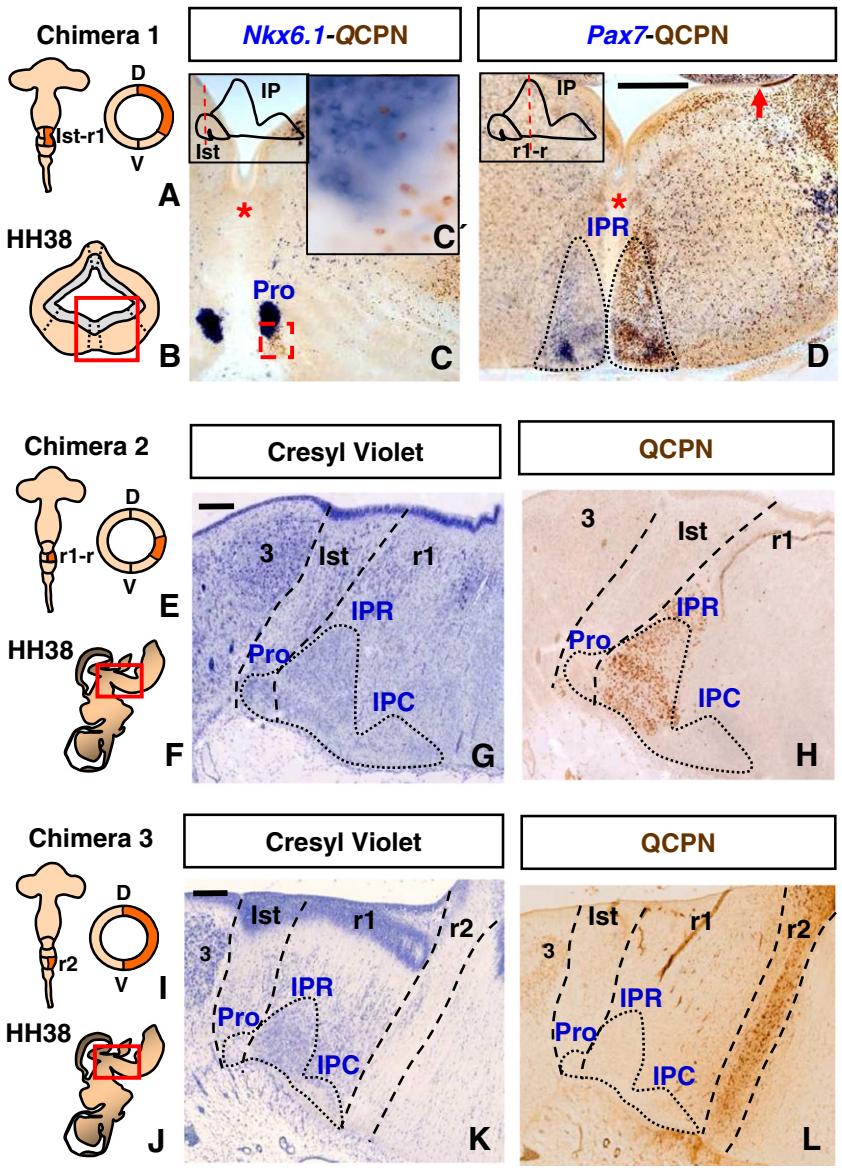

Fig. 4. Quail-chick grafts confirm an isthmic and r1 topography of the IP and its dual alar/basal origin. A–D, Results from quail-chick grafts restricted to the alar plate of both the isthmus and r1 territories (chimera type 1); A,B show schematically the position and dorsoventral extent of the grafted domain (excluding the basal plate), as well as the area shown in the transverse sections obtained at HH38. C,D show cross-sections at the levels indicated in the inset, double-labeled with the QCPN antibody (specific for quail derived cells) and *in situ* probes for *Nkx6.1* or *Pax7*, respectively. C, At the isthmic level, the Pro subnucleus, labeled with *Nkx6.1*, shows absence of grafted quail cells, consistently with a basal plate origin; see enlarged view of the boxed area at the top right corner of C. D, At the level of r1, the IPR shows at the control and grafted sides of the section (left and right, respectively) a very similar pattern of distribution of *Pax7* and QCPN cell populations. Red asterisks indicate the floor plate, and red arrow indicates the alar/basal boundary at the VZ. E–H, Results from quail-chick grafts restricted to a ventral part of the alar plate in rostral r1 (chimera type 2). E,F, Schematic diagrams depicting localization and extent of the graft; the boxed area indicates the sagittally sectioned paramedian region illustrated in G and H. G,H, Adjacent sagittal sections alternatively labeled with cresyl violet (Nissl stain) or QCPN immunoreaction, the latter to show grafted quail tissue. Note the selective and strong labeling of the IPR in a pattern comparable to that shown in Fig. 2G. I–L, Results from quail to chick grafts of an entire half of rhombomere 2 (chimera type 3). I, Diagram showing the extent of the grafted tissue; J, the boxed areas indicate the sagittally sectioned paramedian region illustrated in K and L. K,L, Adjacent sagittal sections at HH38, labeled alternatively with cresyl violet (Nissl stain) or QCPN immunoreaction, to show cytoarchitecture and the grafted quail tissue, respectively. Note that there are no r2-derived quail cells within the IP. Scale bars = 200 μm.

incubated in biotinylated anti-mouse IgG antibody (1:200) in 5% KTBT overnight at 4 °C. The horseradish peroxidase reaction was performed using the avidin–biotin–peroxidase complex (Vectastain ABC kit; Vector Laboratories). HRP detection was carried out using standard diaminobenzidine tetrahydrochloride (DAB) and hydrogen peroxide.

Image analysis

Digital photographs were taken on a Leica microscope (DMR HC) equipped with a Zeiss Axiovision digital camera. Digital images were optimized for contrast and brightness in Adobe PhotoShop (Adobe Systems, San Jose, CA), and figures were mounted and labeled using Microsoft Office PowerPoint.

Results

For description of IP development we systematically used sagittal and transverse sections, the latter strictly oriented according to the oblique topography of r1. This facilitates drawing conclusions about the DV position of the observed cell populations. We empirically found from the literature or previous personal observations that

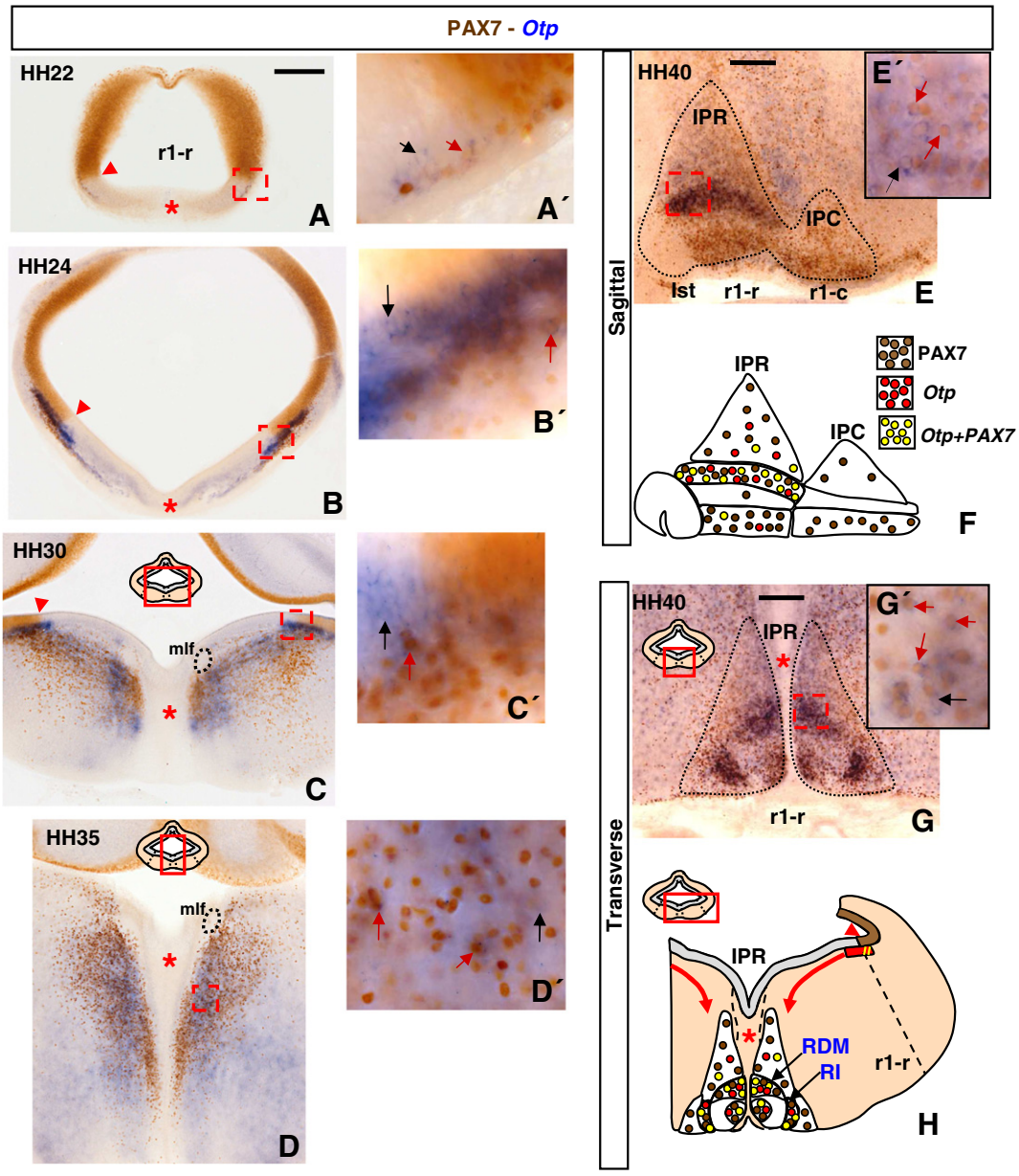

Fig. 5. The *Otp*-positive subpopulations of the IP originate at both sides of the alar–basal boundary of rostral r1. These images illustrate the origin of *Otp*-positive cells and their migration into IP. A–D, Transverse sections double-labeled for PAX7 antibody (brown) and *in situ* hybridization for *Otp* (blue) at HH22, HH24, HH30 and HH35. The areas shown in C–D correspond to the areas boxed in its corresponding inserted diagrams in C and D. Higher magnification of details indicated by boxes in A–D are shown in the insets A′–D′, indicating single *Otp* or double *Otp*-PAX7 labeled cells with black or red arrows, respectively. A,A′, The earliest *Otp*-positive postmitotic cells can be barely observed in the subventricular mantle zone surrounding the alar–basal boundary at HH22. B,B′, At HH24, a more substantial periventricular *Otp* population can be detected at the same location. Note that its alar end coincides with that of the source of migrating PAX7 cells, though only partial PAX7/*Otp* overlap is observed in the alar mantle zone. The *Otp*-positive basal periventricular mantle is as thick as the alar counterpart, whereas a thin stream of labeled cells apparently migrating medialwards appears ventromedially near the basal ventricular zone, mixed with PAX7 cells. C,C′,D,D′, Between HH30 and HH35, the *Otp* cells translocate parallel to the stream of PAX7 cells (partially overlapping them), and the pioneering ones reach the IP. Red asterisks indicate the floor plate. Red arrowheads indicate the alar-basal boundary at the VZ level. E,F, Sagittal section and correlative structural diagram of the IP at HH40; G,H, Transverse section and correlative structural diagram of the IP at HH40. The *Otp*-positive population appears distinctly segregated in different subnuclei of the IPR. Note at higher magnification double-labeled cells (red arrows), but also *Otp*+/PAX7- cells (black arrows), in the respective insets E′,G′. *Otp*-positive cells mainly settle within the RDM and RI subnuclei. F, Tripartite model of the IP, showing the location of cells double-labeled with *Otp* and PAX7, along with those single-labeled for *Otp* or PAX7 (compare E). H, Diagram summarizing the origin, migratory course (red arrow and circles) and final fate of *Otp*-positive cells in the rostral-r1, compared to similarly migrating PAX7 cells (brown circles). Cells coexpressing both markers are depicted as yellow circles. Scale bars = 200 μm.

expression of PAX7, *Nkx6.1*, *Otx2* or *Otp* labeled different IP cell populations. Some of these results were confirmed by fate-mapping experiments using quail-chick homotopic grafts. We used specific reference markers of the isthmus-rhombomere 2 territory. The early isthmus (Ist) was identified by the expression of *Fgf8* (Liu and Joyner, 2001; review in Echevarría et al., 2003; Zervas et al., 2005); alternatively, the isthmic trochlear motor nucleus (4) was labeled by *Phox2a* (Pattyn et al., 1997), and the dopaminergic ventral tegmental area neurons (VTA) in the isthmic and midbrain tegmentum were visualized by the late expression of *Nurr1* (Saucedo-Cardenas et al., 1998). As a landmark of the rhombomere 1 (r1) we used the locus coeruleus, the main noradrenergic nucleus in the brain, which is originated in r1 (LoC; Aroca et al.;, 2006) and is labeled by *Phox2a* (Pattyn et al., 1997) and *Dbh* (dopamine-b-hydroxylase). Finally, we used the

anteriormost expression of *Hoxa2* to visualize the r1-r2 boundary (Prince and Lumsden, 1994; Rijli et al., 1993). Anatomical terminology was adapted from the stereotaxic chick brain atlas of Puelles et al. (2007).

PAX7-positive IP cells originate in alar r1

In an earlier work (Aroca et al., 2006) we first noted that PAX7-positive cells selectively migrated out from the r1 alar plate, entering tangentially the adjacent basal plate. PAX7 signal generally characterizes the alar ventricular zone (VZ) throughout the chicken hindbrain, midbrain and part of pretectum (Fig. 1A,B; Jostes et al., 1990; Ju et al., 2004; Ferrán et al., 2007). In r1 (and nowhere else in the hindbrain) a specific group of mantle derivatives continues to express this marker in the ventralmost sector of the corresponding alar zone (Aroca et al., 2006; present results, Fig. 1G,I). Most of these r1 mantle cells migrate into the basal plate. Here we examined this phenomenon in detail, discovering that one of the targets of this migration was the developing IP complex. We will restrict our description to these cells.

Early phenomena

At HH21 no mantle cells expressed yet PAX7 in the isthmus or r1 (Fig. 1C,D). The first PAX7 positive mantle cells appeared at HH22 (Fig. 5A,A′), and at stage HH24 they are clearly localized specifically at the ventral rim of the r1 alar mantle zone (i.e., adjacent to the alar–basal limit; Fig. 1F). Note that a cross-sections through isthmus-rostral r1 almost lack of such cells (Fig. 1E). By stage HH26, the PAX7 cell population was larger and no longer appeared bounded by the alar–basal limit. Many labeled cells penetrated tangentially the adjacent basal plate mantle (Fig. 1I). The referred migrating population does not overlap with markers of the isthmic mantle such as *Fgf8* (Fig. 1G), or *Nurr1* (Fig. 1K). Similarly, migrating PAX7 cells do not overlap with the r2 mantle zone, identified by expression of *Hoxa2* (Fig. 1G,L). Production of postmitotic PAX7-positive cells at the ventral rim of the r1 alar plate continues at least until HH34 (8 incubation days). They always initiate tangential migratory dispersion oriented exclusively towards the basal plate.

At HH30, the PAX7-positive stream reaches more deeply into the basal plate, always under the ventricular zone, though a number of cells also disperse radially into intermediate levels of the basal territory (Fig. 2A). By stages HH31–34, most PAX7-positive cells appear aggregated in a ventromedial migratory stream, after surrounding the medial longitudinal fascicle (mlf; Fig. 2B; see also 3B,C); this stream now progresses radially ventralwards, parallel to the floor plate. These cells finally reach the prospective subpial locus of the IP at HH35–36 (9–10 incubation days; Fig. 2C,F; see also 3D) and eventually penetrate the median r1 floorplate territory, contributing importantly to the formation of the IP complex (Fig. 2D,E,G-N).

The appearance of a mature morphology of the IP progresses rostrocaudally. In sagittal sections, the rostral IP is first recognizable within the rostral part of r1 at HH36, showing a characteristic apical (dorsal) bulge (IPR; r1-r; Fig. 2F); at this stage the IP primordium is still sparsely populated caudally. The caudal IP appears better defined in the caudal part of r1 at HH39 (IPC; r1-c; Fig. 2G,G′), a stage in which several subdivisions can already be distinguished within each of these rostral and caudal main divisions of the IP.

A tentative model of avian IP subdivisions which roughly agrees with described mammalian ones can be established on the basis of the heterogeneous distribution of PAX7 cells. This model was helpful for mapping the subnuclear distribution of the other IP cell populations expressing different transcription factors. We systematized the IP subdivisions apparent at stage HH39 in sagittal and transverse planes, as shown in Fig. 2G–N. The corresponding terminology is freely adapted from the literature (e.g., Puelles et al., 2007, and mammalian studies; see Discussion).

As was already advanced by Puelles et al. (2007), the avian IP complex is primarily organized in three rostrocaudal divisions, identified as prodromal (Pro), rostral (IPR) and caudal (IPC; Fig. 2G,H). The Pro unit is PAX7-negative and lies in the isthmic floorplate (Fig. 2G,H,I,L). The IPR, lying rostrally within r1, shows *medial and lateral central* parts (RCM, RCL) that are covered by a dorsal shell region with *dorsomedial* and *apical* subnuclei (RDM, RA) and a lateral shell region divided into *intermediate* and *lateral* subnuclei (RI, RL). The abbreviations for all these subdivisions carry an "R" indicating integration within the IPR (Fig. 2H,M). The RCM, RI and RDM units strongly express PAX7, whereas RA has intermediate levels of this signal and RCL is largely PAX7-negative (Fig. 2G,J). The IPC, lying in caudal r1, is also heterogeneous, being composed of *medial* and *lateral central* subnuclei (CCM, CCL), surrounded by apical and lateral shell-like subnuclei (CA, CL). The abbreviations for these subdivisions carry a "C" indicating integration within the IPC (Fig. 2H,N). PAX7 cells predominate in CCM, are scattered in CA and CCL, and seem largely absent in the CL (Fig. 2G,K).

Nkx6.1 positive basal cells in the IP

The transcription factor *Nkx6.1* is known to be expressed in the ventricular zone and mantle of a central domain of the basal plate across the diencephalon, midbrain, and hindbrain (Briscoe et al., 2000; Qiu et al., 1998; Sander et al., 2000). E. Puelles et al. (2001) studied this expression pattern in chick embryos, and showed the existence of *Nkx6.1*-positive cells within the IP. We examined how these cells reach the IP, as well as their detailed topography within the complex, compared to the PAX7-positive population.

There is a uniformly strong ventricular expression of *Nkx6.1* in an intermediate sector of the isthmic and r1 basal plate (Fig. 3A–H); this domain is intercalated dorsoventrally between a lateral *Dbx2*-positive basal domain and the well-known medial basal domain that expresses *Nkx2.2* (the latter lies adjacent to the floor plate; see diagram in Fig. 1B). At HH27, weakly *Nkx6.1*-positive cells were observed subventricularly underneath the strongly positive ventricular patch of the isthmus and rostral r1 (Fig. 3A). Between HH31 and HH34, part of this population spreads radially towards the ventral surface, independently of the ventromedial stream of PAX7 cells (Fig. 3B–C). At HH35, this stream expresses *Nkx6.1* more strongly and gradually converges ventrally and medially with the PAX7 cells at the superficial IP primordium (Fig. 3D,G,H). Observations at later stages indicate that the major target of the *Nkx6.1* cells within IP is the Pro division, where they represent nearly its entire population (Fig. 3E,F,I,J,K), whereas a less dense *Nkx6.1* subpopulation enters selectively the RCL subnucleus, intermixing there with PAX7 cells (Fig. 3I–J,L). These two subgroups probably correspond to distinct isthmic and r1 components of this migration (Fig. 3H,I). Taken together, these data indicate that the IP has at least a dual alar (PAX7-positive) and basal (*Nkx6.1*-positive) origin. The *Nkx6.1* positive populations in the IP represent two independent though longitudinally continuous basal origins. The Pro subnucleus seems to be entirely originated in the isthmus, in a PAX7-negative territory, while the RCL is originated in r1, as suggested by the intermixed PAX7-positive alar subpopulation.

Dual origin of IP cells from alar and basal progenitors is corroborated by quail-chick grafts.

In order to confirm our results about the dual alar–basal origin of PAX7 versus *Nkx6.1* cells of the IP, we performed quail-chick homotopic grafts (Alvarado-Mallart, 1993; Le Douarin, 1993), labeling quail-derived cells with the specific QCPN antibody. We first grafted the alar plate of r1 and isthmus at HH10–11 (approx. 2/3 of the D/V extent of the lateral wall; e.g., chimera 1; Fig. 4A–D). The QCPN-positive IP cells derived from the graft stopped at the border of the prodromal subnucleus, identified by its differential *Nkx6.1* signal (Pro; Fig. 4C,C′). The IPR shows in transverse section a distribution of *Pax7* mRNA signal

comparable to the QCPN-immunoreaction (Fig. 4D). These results support our conclusion about the existence of an alar–basal tangential migration of PAX7 cells and indicate that the origin of the Pro lies outside the alar plate of r1 and isthmus (i.e., is restricted to the basal plate).

To further evaluate the dorsoventral and anteroposterior origin of the PAX7 migratory cells, we selectively grafted the ventral portion of the alar plate of rostral r1 (r1-r; predicted source of IPR) in experiments represented by chimera 2 (Fig. 4E–H). QCPN-reacted sagittal sections at HH38 showed that in this case only the IPR nucleus contained grafted quail cells. The quail cells found within IPR clearly reproduced the IPR subnuclear pattern previously observed with PAX7 immunoreaction (compare Figs. 2G and 4G,H). The Pro subnucleus was unlabeled, as expected, due to its isthmic basal origin. The IPC was similarly unlabeled, supporting its origin in the caudal part of r1 (r1-c). These results suggest that the alar PAX7-cell-generating progenitors of r1-r and r1-c presumably contribute to the IPR and IPC, respectively.

In order to check whether any part of IPC derives from r2 rather than caudal r1, we did quail-chick grafts of the whole D/V extent of r2 at HH10–11 in experiments represented by chimera 3 (Fig. 4I–L). At HH38, the QCPN-labeled territory clearly appeared just caudal to the IPC, supporting the strictly caudal r1 origin of the latter (Fig. 4K,L).

Otp-positive cells in the IP

The transcription factor *Orthopedia* (*Otp*; Simeone et al., 1994) is transiently expressed in chicken embryos in a longitudinal periventricular stripe along the hindbrain between stages HH22–34 (Fig. 5A–C), This well-delimited band of *Otp*-positive cells extends across the alar/basal boundary as defined by PAX7 immunoreaction. The first *Otp*-positive mantle cells appear around stage HH22 (Fig. 5A,A′). At HH24 and HH30 the corresponding subventricular mantle is more densely populated by such cells, which stop dorsally precisely where the PAX7-producing progenitor area ends (Fig. 5B-C; diagram in Fig. 1B). In addition, at HH24 a thin periventricular stream of *Otp*-positive cells extends medialwards, partially overlapping the ventromedial stream of PAX7-positive cells (Fig. 5B). A sizeable proportion of the *Otp* cells therefore partially overlaps with the tangentially migrating alar PAX7-positive elements, though *Otp*-positive/PAX7-negative basal plate derivatives also exist nearby (Fig. 5B,B'). At later stages we observed *Otp*+/PAX7- (black arrows in insets of Fig. 5), *Otp*+/PAX7+ (red arrows in the insets of Fig. 5) and *Otp*-/PAX7+ derivatives in the IP. As observed for the PAX7 cells, *Otp*-positive cells do not accumulate radially near their progenitor areas. Instead they migrate tangentially parallel to (or mixed with) the PAX7-positive ventromedial migratory stream. Once the migrating *Otp* population reaches the paramedian basal plate, most of its cells course radially ventralwards, laterally or overlapping the neighboring PAX7 elements, until they reach the IP (Fig. 5C,D). By HH35, *Otp*-cells are no longer detected close to the alar and basal progenitor regions (Fig. 5D).

The final destination of these *Otp*-positive cells lies mainly within the IPR, where they invade massively the dorsomedial and intermediate subnuclei, with a less important contribution to the central medial subnucleus (RDM, RI, RCM; Fig. 5E–H). The Pro and IPC receive no *Otp*-positive neurons (Fig. 5E,F). As mentioned above, we observed at high magnification that single-labeled PAX7 or *Otp* cells coexist with double labeled *Otp*-PAX7 cells (see insets Fig. 5E′G′).

These data indicate that *Otp*+/PAX7− IP cells possibly originate in the lateral basal plate, adjacent to the alar/basal boundary, whereas *Otp*+/PAX7+ IP cells are probably alar in origin and represent topographically restricted subpopulations within IPR of the previously described alar PAX7-positive cells.

Otx2-positive basal cells in the IP

The transcription factor *Otx2* controls forebrain and midbrain patterning (Acampora and Simeone, 1999; Acampora et al., 2005) and its main expression domain stops caudally in the midbrain, rostral to the isthmic organizer region. There is nevertheless an isolated patch of *Otx2* expression at the rostral hindbrain of the mouse and chick (Simeone and Puelles, unpublished observations) that has not received attention previously as regards its neuronal derivatives or precise neuromeric location. We found that *Otx2* cells eventually appear at the IP, and accordingly examined the origin and possible migration of these cells during development. Postmitotic *Otx2*-positive cells first appeared periventricularly in an intermediate basal plate patch restricted to caudal r1 at HH24 (not shown); this lies under the *Nkx6.1*-positive ventricular zone (Fig. 1B). At HH27, *Otx2*-positive cells relate topographically strictly to a caudal domain of r1, adjacent to the r1–r2 boundary (Fig. 6A), lying thus across the subventricular path of caudal alar PAX7-positive migratory cells (Fig. 6E). Interestingly, we observed at this stage a few *Otx2* cells inside the adjacent ventricular zone, suggesting that the underlying *Otx2* population in the periventricular mantle are originated there (red arrows in Fig. 6A′). At subsequent stages the *Otx2*-positive cells translocate ventromedially through the paramedian basal plate (Fig. 6F), progressively approaching the caudal IP between HH36 and HH39 (Fig. 6B, C,G). Finally, most *Otx2* elements appear aggregated in separate longitudinal clumps along the incipient CCM and CL subnuclei of the IPC, and some dispersed cells are seen also at the CA (Fig. 6D,G,H); note that no such cells were found at the IPR or Pro. At high magnification, scattered PAX7-positive cells appear mixed with the *Otx2* population of IPC, but none of the *Otx2*-expressing cells are immunoreactive for PAX7 (black arrows in Fig. 6B′,C′).

These data demonstrate the existence of a separate basal cell population contributing to the caudal part of the IP complex. A spatially restricted group of basal postmitotic cells express *Otx2*, only at the caudal part of r1. They seem to be originated at the *Nkx6.1*-positive progenitor domain, but, interestingly, they are *Nkx6.1*-negative.

We also investigated other possible dorso-ventral origins for IP subpopulations. For instance, we studied a possible contribution of *Dbx1*/*Dbx2*-positive ventricular cells found across the alar–basal boundary zone (Fig. 1B) or of paramedian *Nkx2.2*-positive progenitor cells (Fig. 1B). However, we found no contribution of *Dbx1*/*Dbx2* or *Nkx2.2*-positive cells to the IP.

Discussion

We have demonstrated that the IP originates and localizes in the isthmus and r1. Its structure contains at least five distinct neuronal subtypes originated in four different dorsoventral progenitor domains. These subpopulations of the IP are characterized by the expression of the transcription factors PAX7, *Otp*, *Nkx6.1* or *Otx2*. We propose a tripartite rostrocaudal model of the IP, with distinct parts in the isthmus, rostral-r1 and caudal-r1. These subdivisions are defined by differential expression of one or more of these transcription factors.

The IP complex originates in the isthmus and r1

Our studies expand previous knowledge of the two main IP parts (IPR, IPC); whereas we show that these two parts arise in molecularly distinct rostral and caudal parts of r1 (Aroca and Puelles, 2005), we also identify a singular third component, the prodromal IP, originated in the isthmus. These results have been verified by fate mapping analysis and contrasted with various molecular markers selective of adjoining neural domains. There is notably no radial or tangential migration contributing to the IP from the midbrain or r2. The *Nkx6.1*-positive *prodromal* subnucleus is entirely originated and located in the isthmus, as we showed with quail/chick chimeras. The PAX7/*Otp*-positive cells (plus some *Nkx6.1* cells) of the IPR mainly originate in rostral-r1. Grafts of this area only labeled the IPR. In contrast, *Otx2*-positive cells are produced selectively at the caudal r1, and represent

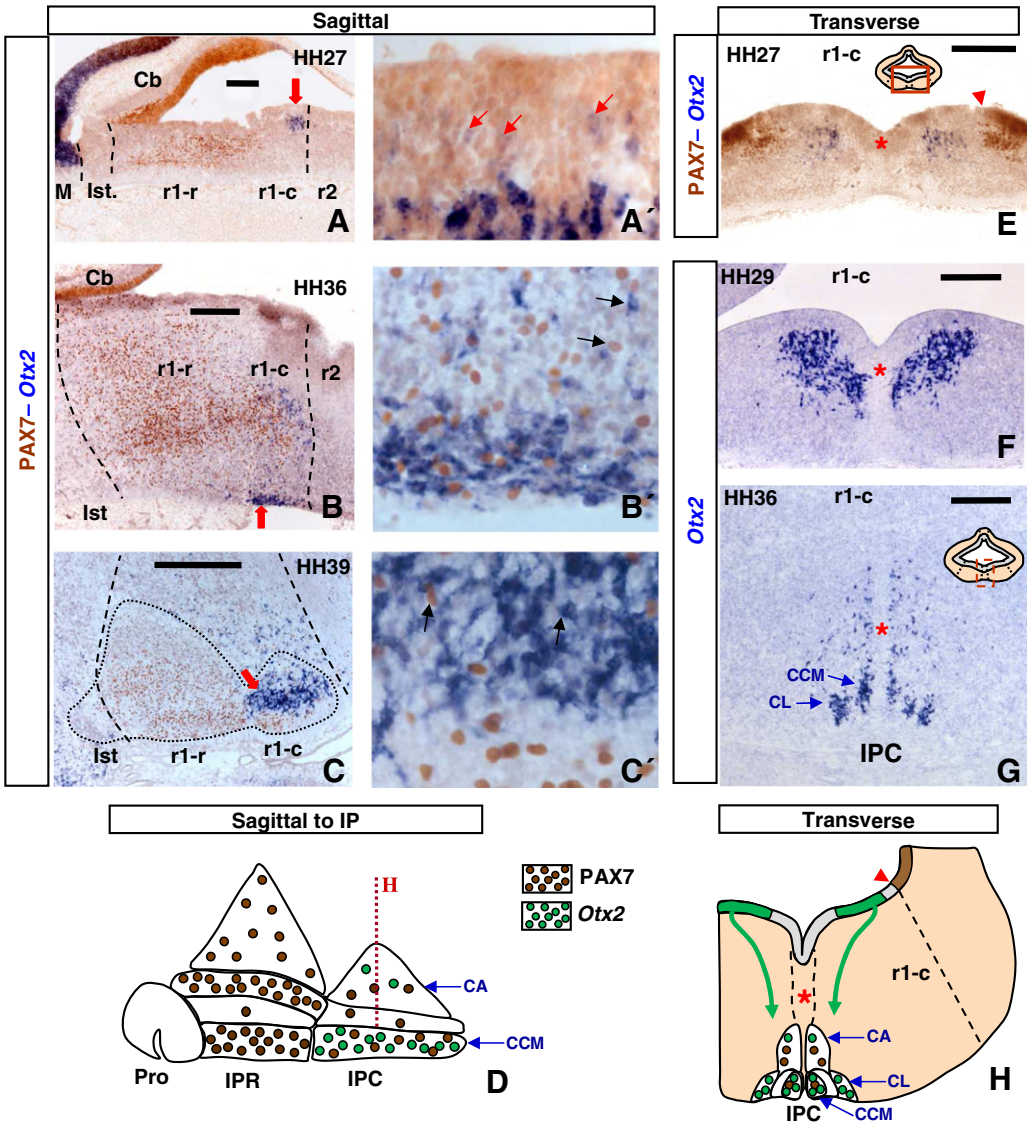

Fig. 6. *Otx2*-positive cells of the caudal IP selectively originate in the intermediate basal plate of caudal r1. A–C, Sagittal sections through r1 showing double labeling with PAX7 antibody (brown) and *in situ* hybridization for *Otx2* (blue) in chick embryos at HH27, HH36 and HH39. A, *Otx2*-positive mantle cells appear in the intermediate basal periventricular zone next to the r1/r2 boundary (note also *Otx2* expression delimiting the caudal midbrain, M, from the isthmus). A′, A higher magnification view of the local ventricular zone (site marked by red arrow in A) shows weak *Otx2* expression in some of its cells (red arrows), suggesting that *Otx2* cells present in the caudal-r1 mantle are produced in the suprajacent basal VZ. B, C, The *Otx2*-positive cells of caudal-r1 subsequently migrate to a subpial position within the caudal IP nucleus. Higher magnification images in B′ and C′ (areas marked with red arrows in B and C) show that the *Otx2*- and PAX7-positive IPC populations are entirely independent (black arrows). D, Sagittal diagram showing the distribution of *Otx2* cells (green) compared to PAX7 cells (brown) in the IP; the former mainly invade the CCM, plus some scattered cells that occupy the CA subdivision. E–G, Transverse sections through caudal-r1 at stages HH27, HH29 and HH36. These images correspond to the area boxed in E. The transverse section shown in E at HH27 was double-labeled with PAX7 antibody (brown) and *in situ* hybridization for *Otx2* (blue). A red arrowhead indicates the A/B boundary; note the intermediate basal position of the early-detected *Otx2* cells. Sections in F and G were processed only for *in situ* hybridization for *Otx2*. Red asterisks indicate the floor plate. At HH29 (F), the basal *Otx2* cells are more numerous and are initiating a ventromedial course of migration (compare with E). At HH36 (G), the migrated population massively enters the IPC, forming the CCM and the CL subnuclei, though some dispersed cells were also found in the CA. H, Schematic cross-section showing the origin, migratory course (green arrow) and final distribution of the *Otx2*-positive basal population in the IPC, compared to PAX7 cells (brown circles). The CCM, CL and CA subnuclei are also indicated (compare with D). Scale bars = 200 μm.

the main population building the IPC, jointly with some PAX7 cells. Control r2 grafts failed to label the IPC, confirming its caudal-r1 origin. Note that Puelles et al. (2007) postulated an r2 IP component, which we reinterpret here as the IPC, formed within caudal-r1.

Classic comparative embryologists and anatomists concluded that the IP belongs to the rostral hindbrain (e.g., Edinger, 1908; Gaupp, 1899; Herrick, 1934; His, 1892; 1895), consistently with our present results. In contrast, the most widely assumed location for the IP in the literature is at the midbrain (e.g., Aizawa et al., 2005; Hanaway et al., 1971; Kuan et al., 2007; Lenn and Bayer, 1986). We believe this error was essentially due to the anatomic tradition to trace the human midbrain-hindbrain limit at the upper border of the pontine bulge (e.g., Dong, 2008; Swanson, 2004, p. 1192). This indeed left the IP, jointly with the whole isthmus and parts of r1 and r2, inside the 'midbrain'. However, the clearcut embryonic caudal midbrain boundary defined by Palmgren (1921) and Vaage (1969, 1973), now understood to be respected in all vertebrates by the caudal limit of expression of the *Otx2* gene in the midbrain, lies rostral to the IP (Echevarría et al., 2003; Hidalgo-Sánchez et al., 2005; Millet et al., 1996). Moreover, some recent authors have misidentified the IP primordium as lying within an area we understand as retromamillary and/or diencephalic tegmentum, wrongly interpreted in its turn as a 'midbrain' tegmental domain (e.g., Bayer and Altman, 2006; see for instance their plate 125D).

Multiple dorsoventral origins of the IP cell populations

In the developing spinal cord distinct subtypes of motoneurons, interneurons or glial cells derive from progenitor domains arranged along the dorsoventral axis of the ventricular zone, each specified differentially by a combinatorial code of transcription factors (Briscoe et al., 1999; Dessaud et al., 2010; Ericson et al., 1997; Hochstim et al., 2008). We have applied the same logic to analyze the developmental construction of the IP in the isthmus and r1.

We observed that the paramedian basal domain of Ist and r1 where *Nkx2.2* is expressed upstream of subsequently produced serotonergic raphe neurons is not involved in the development of the IP (not shown). However, we identified in r1 at least four different progenitor sources for IP neuronal subtypes, marked by the expression of PAX7, *Otp, Nkx6.1* or *Otx2*. An additional source of IP *Nkx6.1* cells was found within the isthmus. The existence in r1 of a subgroup of cells coexpressing PAX7 and *Otp* suggests a possible fifth IP progenitor population, possibly intermixed in a salt-and-pepper pattern with pure PAX7 progenitors in the ventral rim of the alar plate.

Alar origin of IP cells

The transcription factor PAX7 is expressed at early embryonic stages in the proliferating alar ventricular zone in the hindbrain and spinal cord (Jostes et al., 1990). We demonstrated via fate-mapping that a longitudinal band restricted to the ventral rim of the r1 alar plate produces postmitotic PAX7-positive cells that migrate massively into the r1 basal plate. This population generates a *ventromedial* stream of cells migrating tangentially within the basal plate. These ventromedial elements finally reach radially the subpial IP locus and contribute only to the IPR and IPC subnuclei (Fig. 7). The fact that the PAX7-positive migration occurs exclusively in r1 (as opposed to Ist or r2) may be due to restrictive direct or indirect effects at close range of both Fgf8 released from the isthmic organizer and *Hoxa2* expressed in r2 (r1 expresses no *Hox* genes). There was no earlier description in the literature of this alar–basal migratory pathway, nor were alar r1 cells known to contribute importantly to the IP nucleus. Our findings in the chick agree with the reported expression of PAX7 in the adult mouse IP (Stoykova and Gruss, 1994).

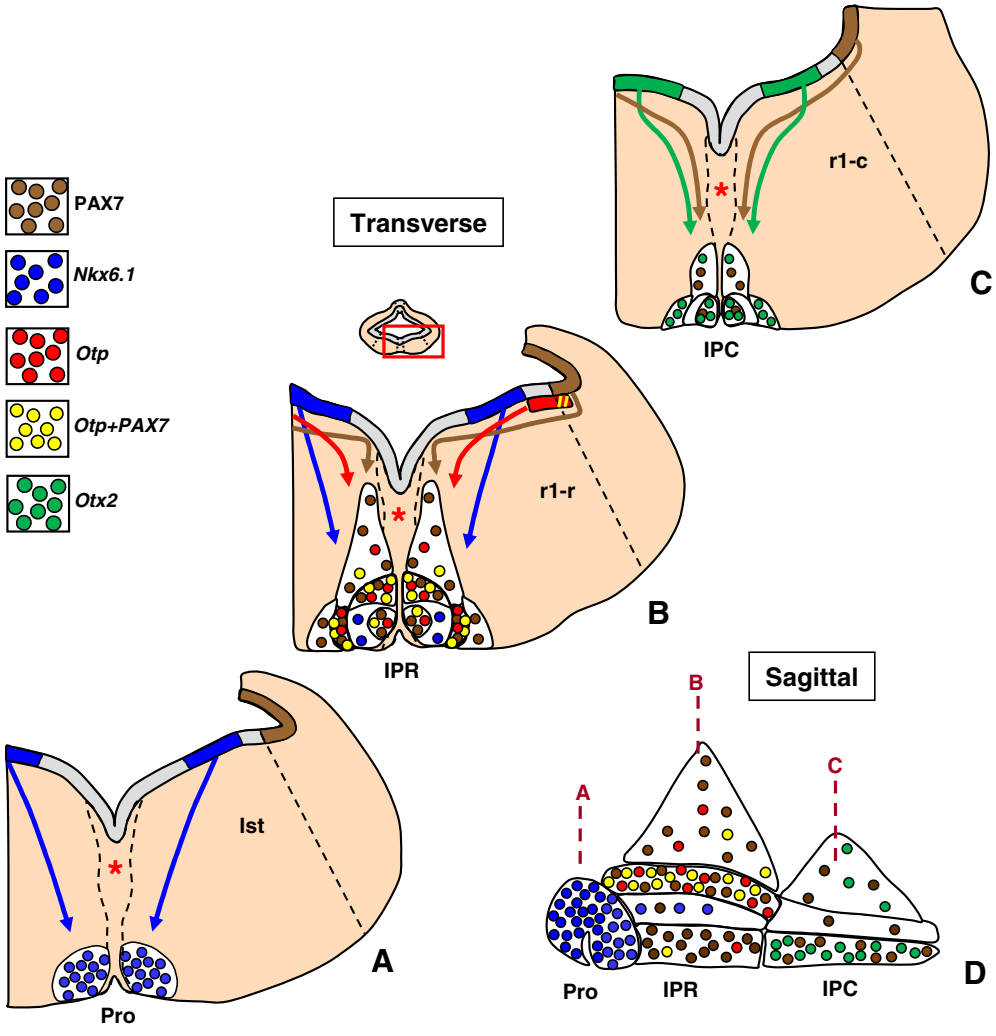

Fig. 7. Schematic model of the diverse anteroposterior and dorsoventral origins of the IP subpopulations within the isthmus and r1 and their final fate in the IP complex. A-C, Schematic diagrams of transverse sections through the IP complex, representing isthmus (Ist), rostral r1 (r1-r) and caudal r1 (r1-c) levels, respectively. The levels of these sections are indicated with red dash-lines in the tripartite sagittal IP model shown in D. Using a color code, we depict differential rostrocaudal and dorsoventral locations of the progenitor domains where PAX7, *Nkx6.1*, and *Otx2* cells arise. A illustrates the isthmic formation of the *Nkx6.1*-positive Pro IP subdivision. In B, the periventricular position is indicated where *Otp* cells first appear, across the alar–basal boundary. The different trajectories followed by the different cell types forming the IP are highlighted with differently colored arrows. The final fate of the five IP subpopulations described in this study is represented with the same color code (colored circles in D). Refer to Fig. 2 (and list of Abbreviations) for the specific names of the IP subnuclei. At least three different subpopulations (labeled with PAX7, PAX7/*Otp*, or *Otp*) populate densely several subnuclei of the IPR (B,D), but leave some subnuclei sparsely populated, suggesting additional as yet unknown populations. The IPC displays at least two distinct subpopulations expressing either PAX7 or *Otx2* (C,D).

The ventral rim of the r1 alar plate produces at least two sorts of PAX7+ cells, one of them being distinguished by the coexpression of *Otp*. The fact that the double-labeled cells enter preferentially the RDM and RI subnuclei of IPR supports their character as a distinct cell type, compared to the PAX7+/*Otp*- cells that invade other IP parts. PAX7-expressing progenitors that generate multiple neuronal subpopulations were recently demonstrated at the olfactory neuroepithelium (Murdoch et al., 2010).

We propose that *Otp*+/PAX7− cells may be generated at the adjacent lateral part of the basal plate. This dual alar plus basal cell production pattern next to the alar–basal boundary coincides with early ventricular expression of the *Dbx1/2* genes bridging the neighboring alar and basal domains. However, our analysis of the developmental expression of *Dbx1/2* in the rostral hindbrain did not disclose *Dbx*-expressing cells in the IP complex. We suspect that the postmitotic lateral basal neurons immediately downregulate *Dbx* gene transcription and activate *Otp* instead.

Basal origins of IP

The basal plate of r1 is divided molecularly into at least three longitudinal zones, provisionally identified as *medial* (paramedian), *intermediate* and *lateral* basal zones.

The medial basal zone is characterized by the expression of *Nkx2.2* downstream of Shh signals, and is the site where serotonergic populations originate (Cheng et al., 2003). However, no IP cells arise from it, according to our mappings (data not shown).

The intermediate basal zone is characterized by the expression of *Nkx6.1*, and this transcription factor plays a role in the specification of neurons (Puelles et al., 2001; Vallstedt et al., 2005). Isthmic intermediate basal-plate-derived *Nkx6.1*-positive cells entirely form the prodromal IP division (Pro), rostral to IPR, whereas *Nkx6.1* cells originated from the r1 intermediate basal plate target the RCL subnucleus of IPR, but none appear at the IPC, suggesting an origin restricted to rostral r1. Previous autoradiographic studies proposed that VTA and IP neurons were originated at the intermediate third of the basal plate of the 'midbrain' (Hanaway et al., 1971). This is consistent with present results on the dorsoventral origin of the *Nkx6.1*-positive IP populations, but the source was localized by us at the isthmus and rostral r1, instead of the midbrain. Interestingly, derivatives of the mouse midbrain *Nkx6.1*-positive progenitor domain do not include the IP nucleus (Prakash et al., 2009).

Otx2 is an essential regulator of the identity, extent and fate of neuronal progenitor domains in the midbrain (E. Puelles et al., 2003, 2004). We demonstrated the existence of a hitherto unknown source of *Otx2*-positive neurons at the intermediate basal zone of the caudal part of r1. These *Otx2* neurons build the mediolateral subdivisions of the IPC, intermixing with dispersed alar PAX7 cells. Further research is needed to explain the regional regulatory processes responsible for the differential formation from dorsoventrally comparable progenitor domains sharing *Nkx6.1* expression of the *Nkx6.1*+/*Otx2* – prodromal IP at the isthmus and rostral r1, whereas *Otx2*+/*Nkx6.1* – IPC cells are generated at the caudal r1. Interestingly, *Nkx6.1* is known to be a repressor of *Otx2* in the midbrain (Prakash et al., 2009).

We had reported previously molecular differences between rostral and caudal parts of r1 (Aroca and Puelles, 2005). These data, as well as present results, are consistent with a cryptic neuromeric subdivision of r1 — such as the r1a and r1b parts suggested by Vaage (1969, 1973). The rostrocaudal histogenetic differences mentioned above imply steplike rostrocaudal patterning effects possibly related causally to differential sensitivity of such units to the gradient of FGF8 signaling spreading from the isthmic organizer (reviewed in Echevarría et al., 2003).

The lateral basal zone of r1 shows ventricular expression of the transcription factors *Dbx1/2* and local subventricular mantle cells express *Otp* (Figs. 1B, 5B). According to the close radial correlation of the *Dbx*-positive progenitors and the *Otp*+/PAX7-negative mantle cells at early stages, the former possibly produce the latter. However, *Dbx1/2* expression disappears as postmitotic cells enter the mantle, which leaves the issue open until *cre*-mediated lineage tracing data are available. Basal *Otp*+/PAX7- cells tend to accumulate at the RDM and RI subnuclei of the IPR, where they are mixed with PAX7+/*Otp*+ double-labeled cells. The topography of the subventricular *Otp* band in the r1 mantle layer, extending like the *Dbx1/2* ventricular bands across the alar–basal boundary, implies a dorsoventral positional patterning effect possibly related to ventral SHH signaling and some opposed dorsalizing effect (Del Giacco et al., 2006). The lack of a similar *Otp*-cell source at the isthmus may reflect local downregulation by strong FGF8 signaling, as occurs in zebrafish (Szabó et al., 2009).

In general, all PAX7-positive components of the IPR and IPC, with or without *Otp*, are migrated alar cells (restricted to r1), whereas the remaining populations come either from the intermediate basal zone (*Nkx6.1*-positive cells rostrally versus *Otx2*-positive cells caudally) or the lateral basal zone (PAX7-negative *Otp*-positive cells). Our data do not exclude that additional progenitor domains may exist for other as yet unidentified IP cell types.

Migration routes of IP cell populations

Here we identify at least four positionally distinct subpopulations of the IP originated at different dorsoventral and rostrocaudal sites across the isthmus and r1. These populations follow different radial or tangential migrations, or a combination of both types of routes to form specific subnuclei of the ipsilateral median and subpial IP complex. We did not observe any cells invading the contralateral side of the IP in our fate mapping experiments.

The longest migration is that of PAX7 cells, which first proceed tangentially medialwards (topologically ventralwards) within the basal plate, later switch to a radial course at the medial basal zone, and finally aggregate subpially at the median floor area. Their behavior suggests repelling or non-permissive conditions for migration within the alar plate, maybe compounded with response to a chemoattractant from the midline. Since the PAX7 cells do not enter the floor plate until they reach a subpial environment, it is possible that the floor plate area may offer to migrating neurons different signals at periventricular, intermediate and subpial levels of the Ist and r1 median raphe.

The intermediate and lateral basal cell populations destined to reach the IP largely migrate via radial routes, which finally also converge medialwards into the median IP formation when they are close to the brain surface. Previous studies showed that the transcription factor *Nkx6.1* is necessary for the correct migration and axonal growth of motoneurons in the hindbrain (Müller et al., 2003; Pattyn et al., 2003).

The IP migratory behaviors discovered by us still await causal explanation in terms of molecular guidance mechanisms. General attracting signals spreading from the hindbrain floor plate have been invoked in various reports unrelated to the IP. Floor plate cells at the ventral midline of the hindbrain express the diffusible protein netrin-1 (Serafini et al., 1996), that represents a bifunctional guidance cue that simultaneously attracts some axons to the floor plate while steering others away. Netrin-1 is a chemorepellent for the trochlear motor axons in the isthmus (Colomarino and Tessier-Lavigne, 1995), but attracts the axons of the superior cerebellar peduncle to their median decussation within the isthmus (Shirasaki et al., 1995). Moreover, netrin 1 is a chemoattractant for the noradrenergic neurons of the locus coeruleus in r1 (Shi et al., 2008), as well as for the inferior olivary and pontine neurons (Bloch-Gallego et al., 1999; Marcos et al., 2009).

The chronology of the arrival of the afferent retroflex tract fibers (from the habenula) at the IP needs to be correlated with these migration patterns. These fibers are well known to perform an unique multiple criss-crossing terminal course within the median IP complex

(Ramon y Cajal, 1909). Accordingly, they must be responding to specific local signals. Interestingly, they express DCC, a netrin-1 receptor (Shu et al., 2000), and Semaphorin 5A, another bifunctional guidance cue (Kantor et al., 2004).

All these general questions about midline signaling affecting the IP probably require definitive answers before we can ask how specific cell types recognize and invade selectively given IP subnuclei.

Similarity of IP structure in model animals

We are inclined to believe that the studied avian IP pattern can be extrapolated, *mutatis mutandis*, to other vertebrates. Molecular mechanisms of brain development are widely conserved in vertebrates. Various aspects of the causal background underpining IP development seem to be plesiomorphic in vertebrates (Nieuwenhuys et al., 1998). For instance, the isthmic secondary organizer (possibly involved in the differential AP identities of the three IP parts), Shh-releasing floor plate (median signaling), alar–basal boundary properties, basal longitudinal zones, and presence of distinct rostral and caudal parts of the IP (plus the habenula, retroflex tract, and other elements of the related circuitry) are all widely conserved features. The isthmic prodromal IP part characterized in the present work (see also Puelles et al., 2007) is probably homologous to the dorsomedial (DM) subnucleus conventionally assigned to the mammalian IPR (e.g., the IPR-DM subnucleus of mammals). This is supported by data found at the Allen Developing Mouse Brain Atlas (developingmouse.brain-map.org) showing a restricted isthmic cell population expressing *netrin G2* (ntnG2) that migrates radially into the 'prodromal' locus of the IP, strictly imitating *Nkx6.1*-expressing cells. These cells acquire postnatally the topography of the DM subnucleus. Using as a reference a standardized rhombomeric tridimensional framework to interpret the brain sections, the usual 'coronal' diagrams for rodent IP subdivisions (e.g., Franklin and Paxinos, 2008; Paxinos and Watson, 1998) result comparable to horizontal or oblique sections through our avian model. Notably, the tendency of the IPC to subdivide into parasagittal strips of cells is manifest in both chick and mouse.

Our present data showing genoarchitectonic heterogeneity of individual IP cell populations invites comparative analysis in other animal forms. Our analysis of relevant literature leads us to think that avian and mammalian IPR and IPC parts correspond to what is wrongly interpreted as *dorsoventral* IP subdivisions in zebrafish (e.g., Aizawa et al., 2005; Gamse et al., 2005).

The mammalian habenula is subdivided into medial and lateral habenula. Only the medial habenula projects to the IP via the retroflex tract (Herkenham and Nauta, 1979). However, the asymmetric habenulae of fish and amphibians are subdivided into dorsal and ventral parts, and the dorsal part projects to the IP (Aizawa et al., 2005). Recent studies have demonstrated that the dorsoventral organization of the zebrafish habenula results from dynamic morphogenetic changes, so that the dorsal and lateral habenula of zebrafish are homologs of the mammalian medial and lateral habenulae, respectively (Amo et al., 2010). This was to be expected in this very conservative neural system, already present in the lamprey and myxine (agnatha), and suggests that some apparent anatomic differences lie more in the eye of the beholder, so to speak, than in nature.

Final remarks

We report here the first detailed developmental study of the IP in any vertebrate species. Our results provide new insight into the reasons of the well-known anatomic complexity of this rostral hindbrain formation, since we propose here novel evidence for dorsoventral (alar and basal) and anteroposterior progenitor domains that separately contribute molecularly diverse cell populations in a specific pattern to the set of subnuclei of the IP complex. The IP is built basically into three rostrocaudal parts across isthmus and rostral and caudal halves of r1, the last two being further subdivided into smaller nuclear units. PAX7-positive progenitors contribute to at least two alar cell lineages with differential final distribution in the IP. *Otp*-positive progenitors can be either basal or alar, in the second case sharing PAX7-expression, and both contribute to the IPR. Along the intermediate basal plate zone, isthmic and rostral r1 progenitors produce *Nkx6.1*-positive Pro and IPR cells, separately from the *Otx2*-positive IPC subpopulations generated at caudal r1 levels. We argued that the differential anteroposterior molecular histogenetic pattern across the IP possibly relates causally to FGF8-mediated signaling from the isthmic organizer.

Our results reveal a singular complexity in the origin of IP component cell populations, which illuminates some of the reasons why this formation is so complex chemoarchitectonically and hodologically. Although the detailed causal reasons for its marked structural, connective and functional heterogeneity still remain obscure, the present data provide us with new conceptual instruments to explore further this mysterious and ancient brain structure.

Abbreviations

3	oculomotor nucleus
4	trochlear nucleus
CA	caudal apical subnucleus of IPC
Cb	cerebellum
CCL	caudal centrolateral subnucleus of IPC
CCM	caudal centromedial subnucleus of IPC
CL	caudal lateral subnucleus of IPC
IP	interpeduncular nucleus
IPC	caudal IP nucleus
IPR	rostral IP nucleus
Ist	isthmus
LoC	locus coeruleus
M	midbrain
MZ	mantle zone
mlf	medial longitudinal fasciculus
Pro	prodromal nucleus of IP
r1	rhombomere 1
r1-c	caudal rhombomere 1
r1-r	rostral rhombomere 1
r2	rhombomere 2
RA	rostral apical subnucleus of IPR
RCL	rostral centrolateral subnucleus of IPR
RCM	rostral centromedial subnucleus of IPR
RDM	rostral dorsomedial subnucleus of IPR
RI	rostral intermediate subnucleus of IPR
RL	rostral lateral subnucleus of IPR
SubC	nucleus subcoeruleus
VTA	ventral tegmental area
VZ	ventricular zone

Acknowledgments

We thank C.R. Mendoza for expert technical assistance. This work was supported by the Spanish Ministry of Science and Innovation (MICINN grants BFU2006-15330-C02-01/BFI to P.A. and BFU2008-04156 to L.P.), FUNDESALUD-PRIS09043 to M.H-S., and SENECA Foundation contract 04548-GERM-06 to L.P (R.C-SM received a scholarship associated with this contract). B.L-C. received a MICINN FPI predoctoral fellowship (BES-2003-1329).

References

Acampora, D., Simeone, A., 1999. The TINS Lecture. Understanding the roles of *Otx1* and *Otx2* in the control of brain morphogenesis. Trends Neurosci. 22, 116–122.

Acampora, D., Annino, A., Tuorto, F., Puelles, E., Lucchesi, W., Papalia, A., Simeone, A., 2005. Otx genes in the evolution of the vertebrate brain. Brain Res. Bull. 66, 410–420.

Aizawa, H., Bianco, I.H., Hamaoka, T., Miyashita, T., Uemura, O., Concha, M.L., Russell, C., Wilson, S.W., Okamoto, H., 2005. Laterotopic representation of left-right information onto the dorso-ventral axis of a zebrafish midbrain target nucleus. Curr. Biol. 15, 238–243.

Alvarado-Mallart, R.M., 1993. Fate and potentialities of the avian mesencephalic/metencephalic neuroepithelium. J. Neurobiol. 24, 1341–1355.

Amo, R., Aizawa, H., Takahoko, M., Kobayashi, M., Takahashi, R., Aoki, T., Okamoto, H., 2010. Identification of the zebrafish ventral habenula as a homolog of the mammalian lateral habenula. J. Neurosci. 30, 1566–1574.

Aroca, P., Puelles, L., 2005. Postulated boundaries and differential fate in the developing rostral hindbrain. Brain Res. Brain Res. Rev. 49, 179–190.

Aroca, P., Lorente-Canovas, B., Mateos, F.R., Puelles, L., 2006. Locus coeruleus neurons originate in alar rhombomere 1 and migrate into the basal plate: studies in chick and mouse embryos. J. Comp. Neurol. 496, 802–818.

Bayer, S.A., Altman, J., 2006. Atlas of human central nervous system development. Vol. IV. The Human Brain during the Late First Trimester. Taylor & Francis Press, London.

Bloch-Gallego, E., Ezan, F., Tessier-Lavigne, M., Sotelo, C., 1999. Floor plate and netrin-1 are involved in the migration and survival of inferior olivary neurons. J. Neurosci. 19, 4407–4420.

Boardman, P.E., Sanz-Ezquerro, J., Overton, I.M., Burt, D.W., Bosch, E., Fong, W.T., Ticle, C., Brown, W.R., Wilson, S.A., Hubbard, S.J., 2002. A comprehensive collection of chicken cDNA. Curr. Biol. 12, 1965–1969.

Briscoe, J., Sussel, L., Serup, P., Hartigan-O'Connor, D., Jessell, T.M., Rubenstein, J.L., Ericson, J., 1999. Homeobox gene *Nkx2.2* and specification of neuronal identity by graded Sonic hedgehog signalling. Nature 398, 622–627.

Briscoe, J., Pierani, A., Jessell, T.M., Ericson, J., 2000. A homeodomain protein code specifies progenitor cell identity and neuronal fate in the ventral neural tube. Cell 10, 435–445.

Briscoe, J., Ericson, J., 2001. Specification of neuronal fates in the ventral neural tube. Curr. Opin. Neurobiol. 11, 43–49.

Cheng, L., Chen, C.L., Tan, M., Qiu, M., Johnson, J., Ma, Q., 2003. *Lmx1b*, *Pet-1*, and *Nkx2.2* coordinately specify serotonergic neurotransmitter phenotype. J. Neurosci. 23, 9961–9967.

Colomarino, S.A., Tessier-Lavigne, M., 1995. The axonal chemoattractant Netrin-1 is also a chemorepellent for trochlear motor axons. Cell 81, 621–629.

Contestabile, A., Flumerfelt, B.A., 1981. Afferent connections of the interpeduncular nucleus and the topographic organization of the habenular-interpeduncular pathway, an HRP study in the rat. J. Comp. Neurol. 196, 53–270.

Del Giacco, L., Sordino, P., Pistocchi, A., Andreakis, N., Tarallo, R., Di Benedetto, B., Cotelli, F., 2006. Differential regulation of the zebrafish *orthopedia* I gene during fate determination of diencephalic neurons. BMC Dev. Biol. 6, 50.

Dessaud, E., Ribes, V., Balaskas, N., Yang, L., Pierani, A., Kicheva, A., Novitch, B.G., Briscoe, J., Sasai, N., 2010. Dynamic assignment and maintenance of positional identity in the ventral neural tube by the morphogen *sonic hedgehog*. PLoS Biol. 8, 1–14.

Dong, H., 2008. The Allen Reference Atlas. Wiley, Hoboken.

Echevarría, D., Vieira, C., Gimeno, L., Martínez, S., 2003. Neuroepithelial secondary organizers and cell fate specification in the developing brain. Brain Res. Brain Res. Rev. 43, 179–191.

Edinger, L., 1908. Vorlesungen über den Bau der nervösen Zentralorgane des Menschen und der Tiere. Bd. II, Vergleichende Anatomie des Gehirns7th edition. Vogel, Leipzig.

Ericson, J., Rashbas, P., Schedl, A., Brenner-Morton, S., Kawakami, A., van Heynengen, V., Jessell, T.M., Briscoe, J., 1997. Pax6 controls progenitor cell identity and neuronal fate in response to graded Shh signaling. Cell 90, 169–180.

Ferraguti, F., Zoli, M., Aronsson, M., Agnati, L.F., Goldstein, M., Filer, D., Fuxe, K., 1990. Distribution of *glutamic acid decarboxylase* messenger RNA-containing nerve cell populations of the male rat brain. J. Chem. Neuroanat. 3, 377–396.

Ferrán, J.L., Sánchez-Arrones, L., Sandoval, J.E., Puelles, L., 2007. A model of early molecular regionalization in the chicken embryonic pretectum. J. Comp. Neurol. 505, 379–403.

Franklin, K.B.J., Paxinos, G., 2008. The Mouse Brain in Stereotaxic Coordinates, 3rd ed. Elsevier, Amsterdam.

Gamse, J.T., Kuan, Y.S., Macurak, M., Brösamle, C., Thisse, B., Thisse, C., Halpern, M.E., 2005. Directional asymmetry of the zebrafish epithalamus guides dorsoventral innervation of the midbrain target. Development 132, 4869–4881.

Gaupp, E., 1899. Lehre vom Nervensystem. In: Ecker, A., Wiedersheim, M.R. (Eds.), Anatomie des Frosches. Braunschweig.

Groenewegen, H.J., Ahlenius, S., Haber, S.N., Kowall, N.W., Nauta, W.J.H., 1986. Cytoarchitecture, fiber connections, and some histochemical aspects of the interpeduncular nucleus in the rat. J. Comp. Neurol. 249, 65–102.

Hamburger, V., Hamilton, H.L., 1951. A series of normal stages in the development of the chick embryo. J. Morphol. 88, 49–92.

Hamill, G.S., Olschowka, J.A., Lenn, N.J., Jacobowitz, D.M., 1984. The subnuclear distribution of substance P, cholecystokinin, vasoactive intestinal peptide, somatostatin, leu-enkephalin, DBH and serotonin in the rat interpeduncular nucleus. J. Comp. Neurol. 226, 580–596.

Hamill, G.S., Lenn, N.J., 1984. The subnuclear organization of the rat interpeduncular nucleus: a light and electron microscopic study. J. Comp. Neurol. 222, 396–408.

Hanaway, J., McConnell, J.A., Netsky, M.G., 1971. Histogenesis of the substantia nigra, ventral tegmental area of Tsai and interpeduncular nucleus: an autoradiographic study of the mesencephalon in the rat. J. Comp. Neurol. 142, 59–73.

Hemmendinger, L.M., Moore, R.Y., 1984. Interpeduncular nucleus organization in the rat. Cytoarchitecture and histochemical analysis. Brain Res. Bull. 13, 163–179.

Herkenham, M., Nauta, W.J., 1979. Efferent connections of the habenular nuclei in the rat. J. Comp. Neurol. 187, 19–47.

Herrick, C.J., 1934. The interpeduncular nucleus of the brain of Necturus. J. Comp. Neurol. 60, 111–136.

Hidalgo-Sánchez, M., Millet, S., Bloch-Gallego, E., Alvarado-Mallart, R.M., 2005. Specification of the meso-isthmo-cerebellar region: the *Otx2*/*Gbx2* boundary. Brain Res. Brain Res. Rev. 49, 134–149.

Hikosaka, O., 2010. The habenula: from stress evasion to value-based decision-making. Nat. Neurosci. 11, 503–513.

His, W., 1892. Zur allgemeinen Morphologie des Gehirns. Arch. Anat. Entw. Gesch. 1892, 346–383.

His, W., 1895. Die Anatomische Nomenclatur. Nomina Anatomica. Suppl. Bd. Arch. Anat. Entw. Gesch. 1895, 155–177.

Hochstim, C., Deneen, B., Lukaszewicz, A., Zhou, Q., Anderson, D.J., 2008. Identification of positionally distinct astrocyte subtypes whose identities are specified by a homeodomain code. Cell 133, 510–522.

Ives, W.R., 1971. The interpeduncular complex of selected rodents. J. Comp. Neurol. 141, 77–94.

Jessell, T.M., 2000. Neuronal specification in the spinal cord: inductive signals and transcriptional codes. Nat. Rev. Genet. 1, 20–29.

Jostes, B., Walther, C., Gruss, P., 1990. The murine paired box gene *Pax7* is expressed specifically during the development of the nervous and muscular system. Mech. Dev. 33, 27–37.

Ju, M.J., Aroca, P., Luo, J., Puelles, L., Redies, C., 2004. Molecular profiling indicates avian branchiomotor nuclei invade the hindbrain alar plate. Neuroscience 128, 785–796.

Kantor, D.B., Chivatakarn, O., Peer, K.L., Oster, S.F., Inatani, M., Hansen, M.J., Flanagan, J.G., Yamaguchi, Y., Sretavan, D.W., Giger, R.J., Kolodkin, A.L., 2004. Semaphorin 5A is a bifunctional axon guidance cue regulated by heparan and chondroitin sulfate proteoglycans. Neuron 44, 961–975.

Klemm, W.R., 2004. Habenular and interpeduncularis nuclei: shared components in multiple-function networks. Med. Sci. Monit. 10, 261–273.

Kuan, Y.S., Gamse, J.T., Schreiber, A.M., Halpern, M.E., 2007. Selective asymmetry in a conserved forebrain to midbrain projection. J. Exp. Zool. B Mol. Dev. Evol. 308, 669–678.

Le Douarin, N.M., 1993. Embryonic neural chimeras in the study of brain development. Trends Neurosci. 16, 64–72.

Lenn, N.J., Bayer, S.A., 1986. Neurogenesis in subnuclei of the rat interpeduncular nucleus and medial habenula. Brain Res. Bull. 16, 219–224.

Liu, A., Joyner, A.L., 2001. Early anterior/posterior patterning of the midbrain and cerebellum. Annu. Rev. Neurosci. 24, 869–896.

Marcos, S., Backer, S., Causeret, F., Tessier-Lavigne, M., Bloch-Gallego, E., 2009. Differential roles of Netrin-1 and its receptor DCC in inferior olivary neuron migration. Mol. Cell. Neurosci. 41, 429–439.

Millet, S., Bloch-Gallego, E., Simeone, A., Alvarado-Mallart, R.M., 1996. The caudal limit of *Otx2* gene expression as a marker of the midbrain/hindbrain boundary: a study using *in situ* hybridisation and chick/quail homotopic grafts. Development 122, 3785–3797.

Müller, M., Jabs, N., Lorke, D.E., Fritzsch, B., Sander, M., 2003. Nkx6.1 controls migration and axon pathfinding of cranial branchio-motoneurons. Development 130, 5815–5826.

Murdoch, B., DelConte, C., García-Castro, M.I., 2010. Embryonic Pax7-expressing progenitors contribute multiple cell types to the postnatal olfactory epithelium. J. Neurosci. 30, 9523–9532.

Nieto, M.A., Patel, K., Wilkinson, D.G., 1996. *In situ* hybridization analysis of chick embryos in whole mount and tissue sections. Methods Cell Biol. 51, 219–235.

Nieuwenhuys, R., Ten, Donkelaar H.J., Nicholson, C., 1998. The Central Nervous System of Vertebrates. Vol. I, 1st ed. Springer, Berlin, Heidelberg, New York.

Nieuwenhuys, R., Voogd, J., Van Huijzen, C., 2008. The Human Central Nervous System, 4th ed. Springer, Berlin, Heidelberg, New York.

Palmgren, A., 1921. Embryological and morphological studies on the midbrain and cerebellum of vertebrates. Acta Zool. 2, 1–94.

Panigrahy, A., Sleeper, L.A., Assmann, S., Rava, L.A., White, W.F., Kinney, H.C., 1998. Developmental changes in heterogeneous patterns of neurotransmitter receptor binding in the human interpeduncular nucleus. J. Comp. Neurol. 390, 322–332.

Pattyn, A., Morin, X., Cremer, H., Goridis, C., Brunet, J.F., 1997. Expression and interactions of the two closely related homeobox genes *Phox2a* and *Phox2b* during neurogenesis. Development 124, 4065–4075.

Pattyn, A., Vallstedt, A., Dias, J.M., Samad, O.A., Krumlauf, R., Rijli, F.M., Brunet, J.F., Ericson, J., 2003. Coordinated temporal and spatial control of motor neuron and serotonergic neuron generation from a common pool of CNS progenitors. Genes Dev. 15, 729–737.

Paxinos, G., Watson, C., 1998. The Rat Brain in Stereotaxic Coordinates, 6th ed. Elsevier.

Prakash, N., Puelles, E., Freude, K., Trümbach, D., Omodei, D., Di Salvio, M., Sussel, L., Ericson, J., Sander, M., Simeone, A., Wurst, W., 2009. *Nkx6.1* controls the identity and fate of red nucleus and oculomotor neurons in the mouse midbrain. Development 136, 2545–2555.

Prince, V., Lumsden, A., 1994. Hoxa-2 expression in normal and transposed rhombomeres: independent regulation in the neural tube and neural crest. Development 120, 911–923.

Puelles, E., Rubenstein, J.L., Puelles, L., 2001. Chicken *Nkx6.1* expression at advanced stages of development identifies distinct brain nuclei derived from the basal plate. Mech. Dev. 102, 279–282.

Puelles, E., Acampora, D., Lacroix, E., Signore, M., Annino, A., Tuorto, F., Filosa, S., Corte, G., Wurst, W., Ang, S.L., Simeone, A., 2003. *Otx* dose-dependent integrated control of antero-posterior and dorso-ventral patterning of midbrain. Nat. Neurosci. 6, 453–460.

Puelles, E., Annino, A., Tuorto, F., Usiello, A., Acampora, D., Czerny, T., Brodski, C., Ang, S.L., Wurst, W., Simeone, A., 2004. *Otx2* regulates the extent, identity and fate of neuronal progenitor domains in the ventral midbrain. Development 131, 2037–2048.

Puelles, L., Martinez-de-la-Torre, M., Paxinos, G., Watson, C., Martínez, S., 2007. The Chick Brain in Stereotaxic Coordinates. An Atlas featuring Neuromeric Subdivisions and Mammalian Homologies. Elsevier, Academic Press, New York.

Quina, L.A., Wang, S., Ng, L., Turner, E.E., 2009. *Brn3a* and *Nurr1* mediate a gene regulatory pathway of habenula development. J. Neurosci. 29, 14309–14322.

Qiu, M., Shimamura, K., Sussel, L., Chen, S., Rubenstein, J.L., 1998. Control of anteroposterior and dorsoventral domains of *Nkx6.1* gene expression relative to other *Nkx* genes during vertebrate CNS development. Mech. Dev. 72, 77–88.

Rijli, F.M., Mark, M., Lakkaraju, S., Dierich, A., Dollé, P., Chambon, P., 1993. A homeotic transformation is generated in the rostral branchial region of the head by disruption of Hoxa-2, which acts as a selector gene. Cell 75, 1333–1349.

Ramon y Cajal, S., 1909. Histologie du Systeme Nerveux de 1'Homme et des Vertebres, L. Azoulay, transl. 2, 270–275, Maloine, Paris.

Sander, M., Paydar, S., Ericson, J., Briscoe, J., Berber, E., German, M., Jessell, T.M., Rubenstein, J.L., 2000. Ventral neural patterning by *Nkx* homeobox genes: Nkx6.1 controls somatic motor neuron and ventral interneuron fates. Genes Dev. 14, 2134–2139.

Saucedo-Cardenas, O., Quintana-Hau, J.D., Le, W.D., Smidt, M.P., Cox, J.J., De Mayo, F., Burbach, J.P.H., Conneely, O.M., 1998. *Nurr1* is essential for the induction of the dopaminergic phenotype and the survival of ventral mesencephalic late dopaminergic precursor neurons. PNAS 95, 4013–4018.

Serafini, T., Colamarino, S.A., Leonardo, E.D., Wang, H., Beddington, R., Skarnes, W.C., Tessier-Lavigne, M., 1996. Netrin-1 is required for commissural axon guidance in the developing vertebrate nervous system. Cell 87, 1001–1014.

Shi, M., Guo, C., Dai, J.X., Ding, Y.Q., 2008. DCC is required for the tangential migration of noradrenergic neurons in locus coeruleus of mouse brain. Mol. Cell. Neurosci. 39, 529–538.

Shibata, H., Suzuki, T., 1984. Efferent projections of the interpeduncular complex in the rat, with special reference to its subnuclei: a retrograde horseradish peroxidase study. Brain Res. 296, 345–349.

Shirasaki, R., Tamada, A., Katsumata, R., Murakami, F., 1995. Guidance of cerebellofugal axons in the rat embryo: directed growth toward the floor plate and subsequent elongation along the longitudinal axis. Neuron 14, 961–972.

Shirasaki, R., Pfaff, S.L., 2002. Transcriptional codes and the control of neuronal identity. Annu. Rev. Neurosci. 25, 251–281.

Shu, T., Valentino, K.M., Seaman, C., Cooper, H.M., Richards, L.J., 2000. Expression of the netrin-1 receptor, deleted in colorectal cancer (DCC), is largely confined to projecting neurons in the developing forebrain. J. Comp. Neurol. 416, 201–212.

Shinoda, K., Michigami, T., Awano, K., Shiotani, Y., 1988. Analysis of the rat interpeduncular subnuclei by immunocytochemical double-staining for enkephalin and substance P, with some reference to the coexistence of both peptides. J. Comp. Neurol. 271, 243–256.

Simeone, A., D'Apice, M.R., Nigro, V., Casanova, J., Graziani, F., Acampora, D., Avantaggiato, V., 1994. *Orthopedia*, a novel homeobox-containing gene expressed in the developing CNS of both mouse and Drosophila. Neuron 13, 83–101.

Stoykova, A., Gruss, P., 1994. Roles of *Pax*-genes in developing and adult brain as suggested by expression patterns. J. Neurosci. 14, 1395–1412.

Swanson, L.W., 2004. Brain Maps: Structure of the Rat Brain, 3rd ed. Elsevier Academic Press, Oxford.

Szabó, N.E., Zhao, T., Cankaya, M., Theil, T., Zhou, X., Alvarez-Bolado, G., 2009. Role of neuroepithelial *Sonic hedgehog* in hypothalamic patterning. J. Neurosci. 29, 6989–7002.

Vaage, S., 1969. Segmentation of the primitive neural tube in chick embryos. Ergeb. Anat. Entwicklungsgesch. 41, 1–88.

Vaage, S., 1973. The histogenesis of the isthmic nuclei in chick embryos (*Gallus domesticus*). Z. Anat. Entwicklungsgesch. 142, 283–314.

Vallstedt, A., Klos, J.M., Ericson, J., 2005. Multiple dorsoventral origins of oligodendrocyte generation in the spinal cord and hindbrain. Neuron 45, 55–67.

Zervas, M., Blaess, S., Joyner, A.L., 2005. Classical embryological studies and modern genetic analysis of midbrain and cerebellum development. Curr. Top. Dev. Biol. 69, 101–138.

Ziehen, T., 1906. Die Morphogenie des Zentralnervensystems der Säugetiere. Hertwig Hb.d. vergl. u. Exp. Entwicklungslehre der Wirbeltiere, Bd. 2 Fischer, Jena.